Impact and mitigation of disruptions with the ITER-like wall in JET

M. Lehnen
and JET EFDA contributors
24th IAEA Fusion Energy Conference 2012

ITER-like wall

The choice of material of plasma facing components affects

- heat load capability
- disruption process

main chamber ***beryllium***

heat load limit: ~25 $MJm^{-2}s^{-0.5}$
low radiation efficiency

divertor ***tungsten***

heat load limit: ~50 $MJm^{-2}s^{-0.5}$
high radiation efficiency

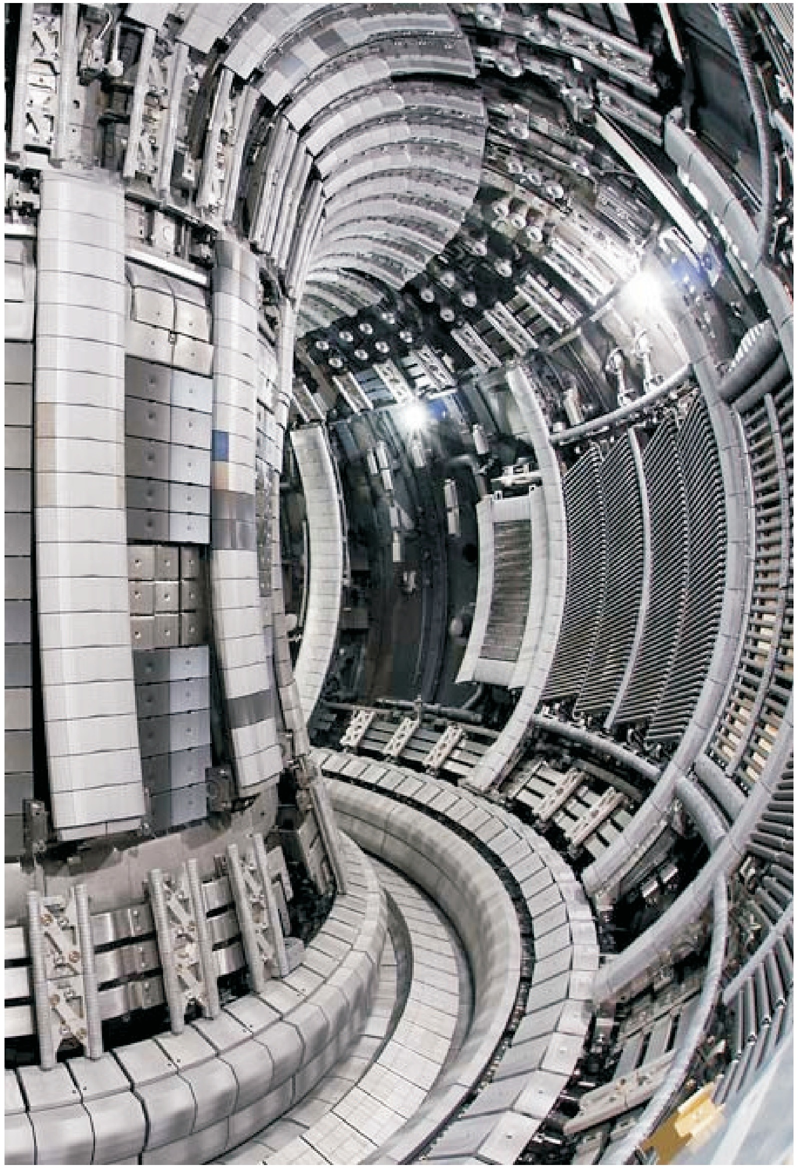

Carbon wall

The choice of material of plasma facing components affects

- heat load capability
- disruption process

all components ***carbon***

heat load limit: ~50 $MJm^{-2}s^{-0.5}$

high radiation efficiency

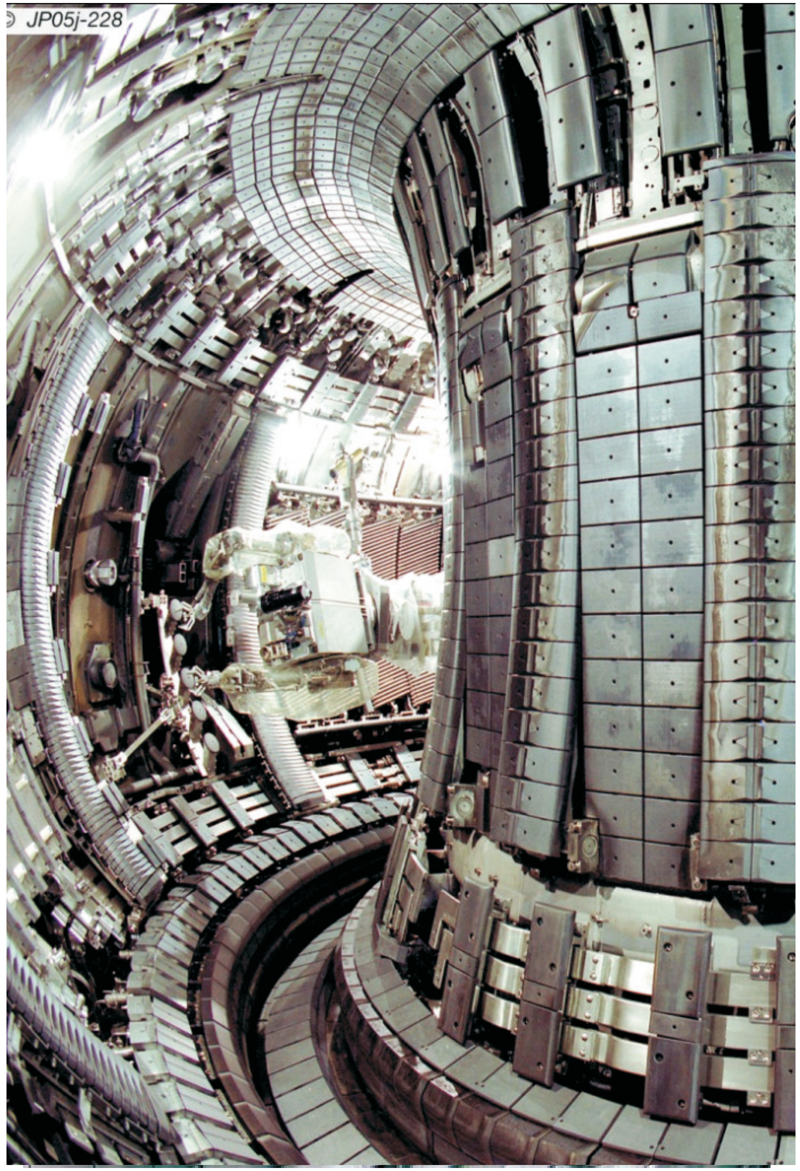

Disruption in a nutshell

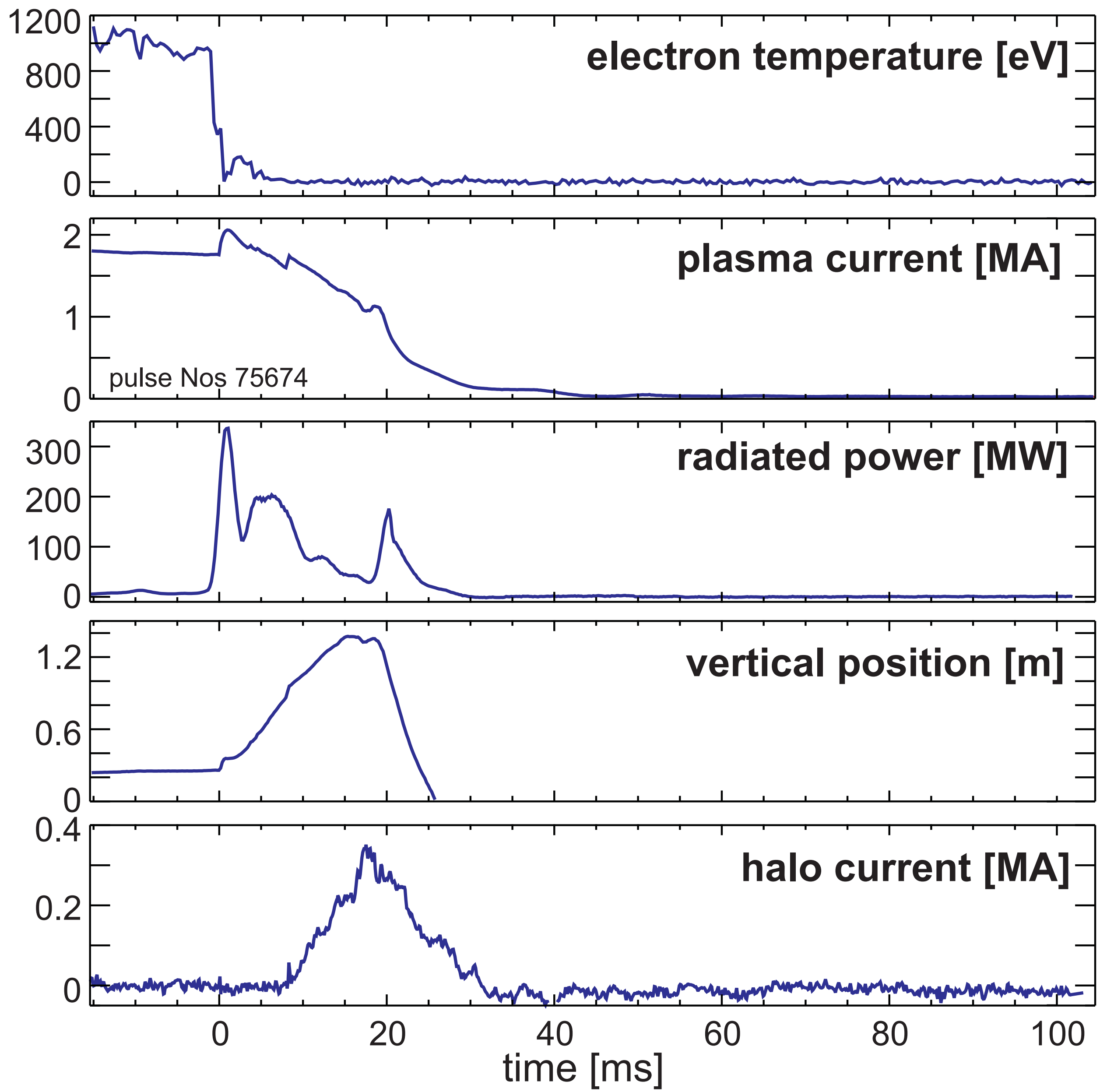

Carbon wall

fast thermal quench

fast current decay

high radiation up to GW range

vertical displacement

halo currents

Disruption in a nutshell

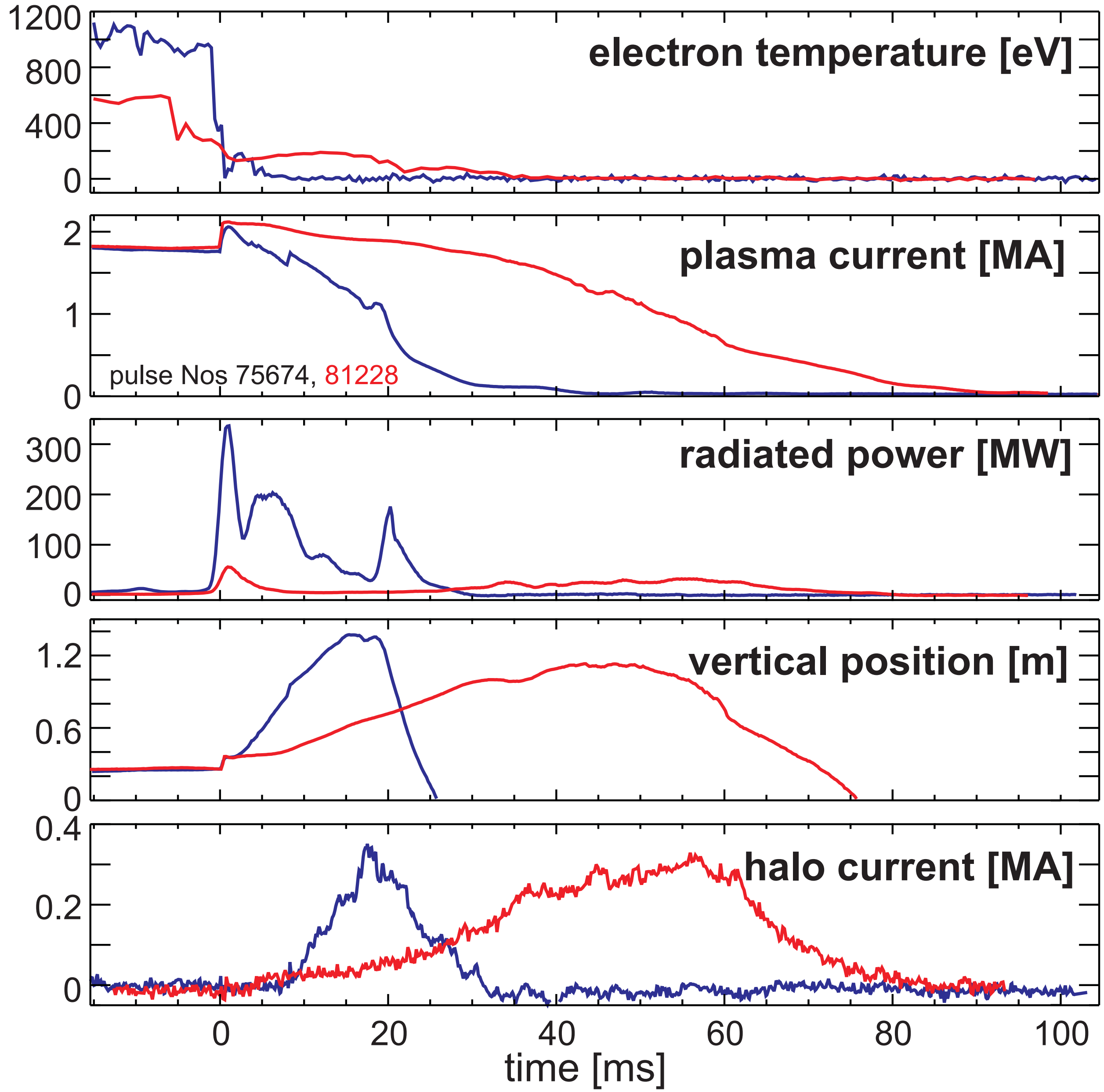

ITER-like wall

hot CQ plasma

slow current decay

low radiation several 10MW only

slower vertical displacement

longer halo current phase

Outline

The fundamental change with the **new ITER-like wall** is the **absence of radiating impurities** during the disruption process.

Outline

- *energy balance and role of radiation*
- *time scales (current quench)*
- *electro-magnetic loads*
- *heat loads*

- *mitigation by massive gas injection*

Energy balance

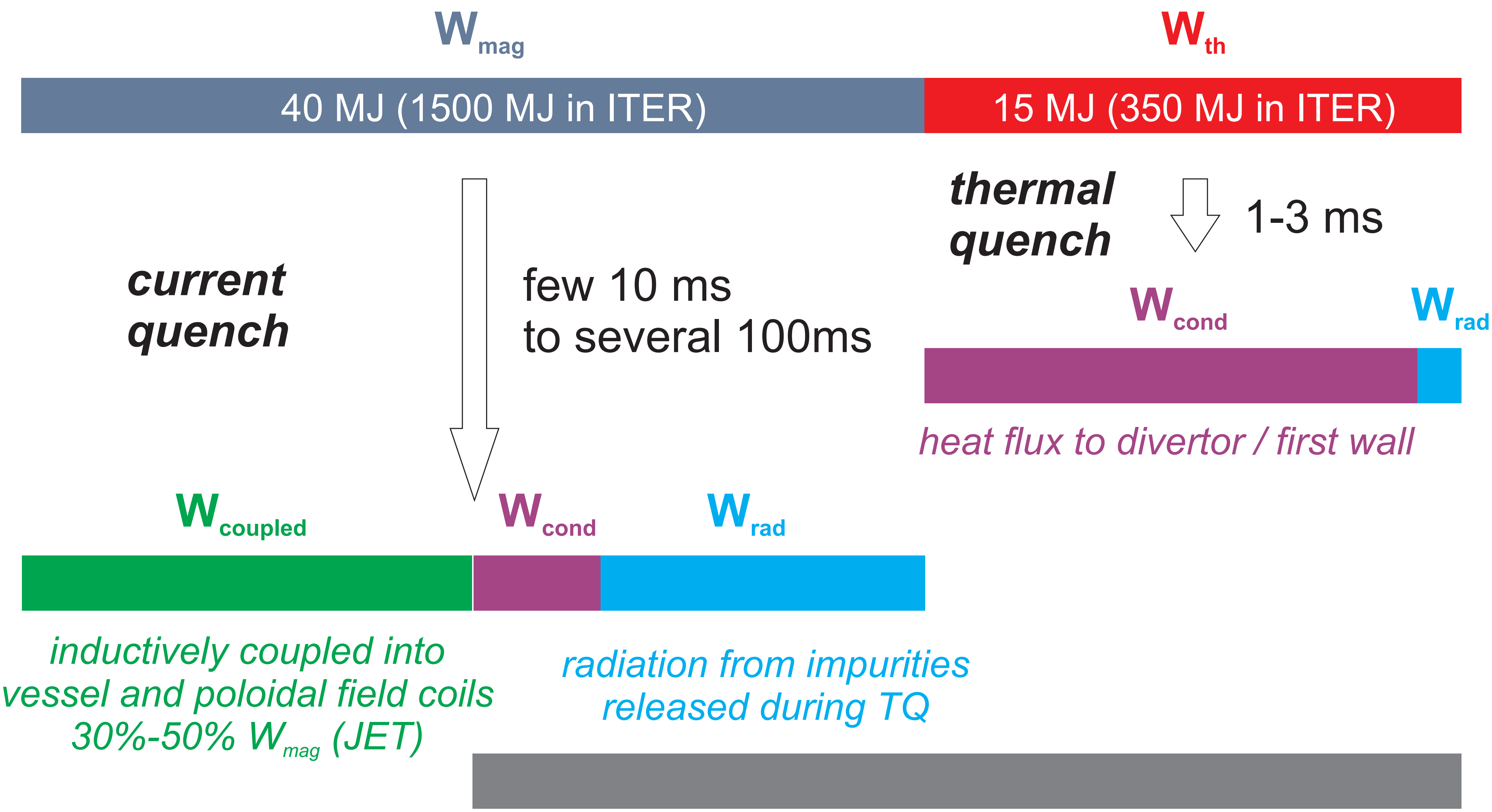

$$W_{plasma} = W_{mag} + W_{th} - W_{coupled}$$

Radiation

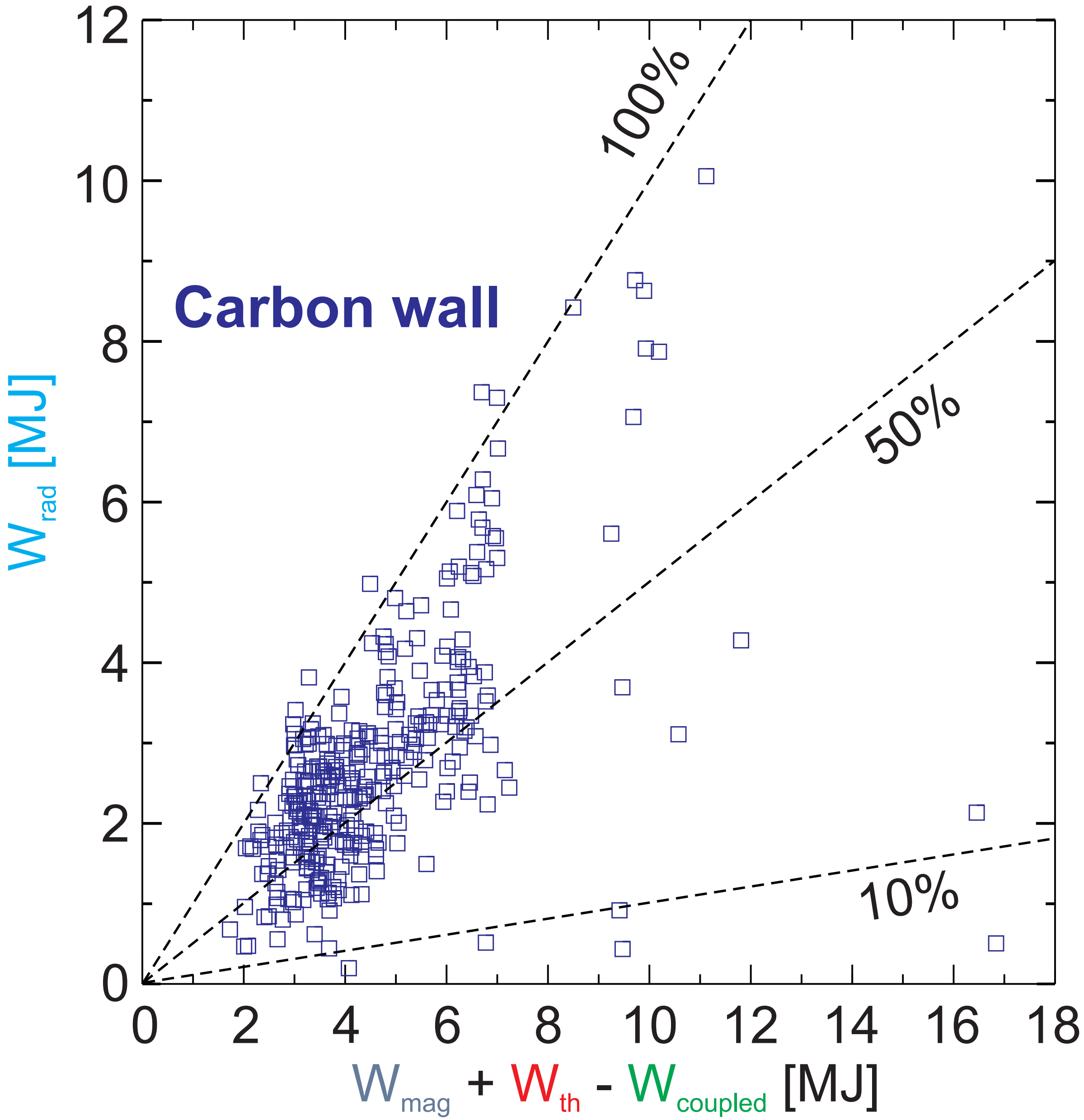

Carbon wall

Radiation

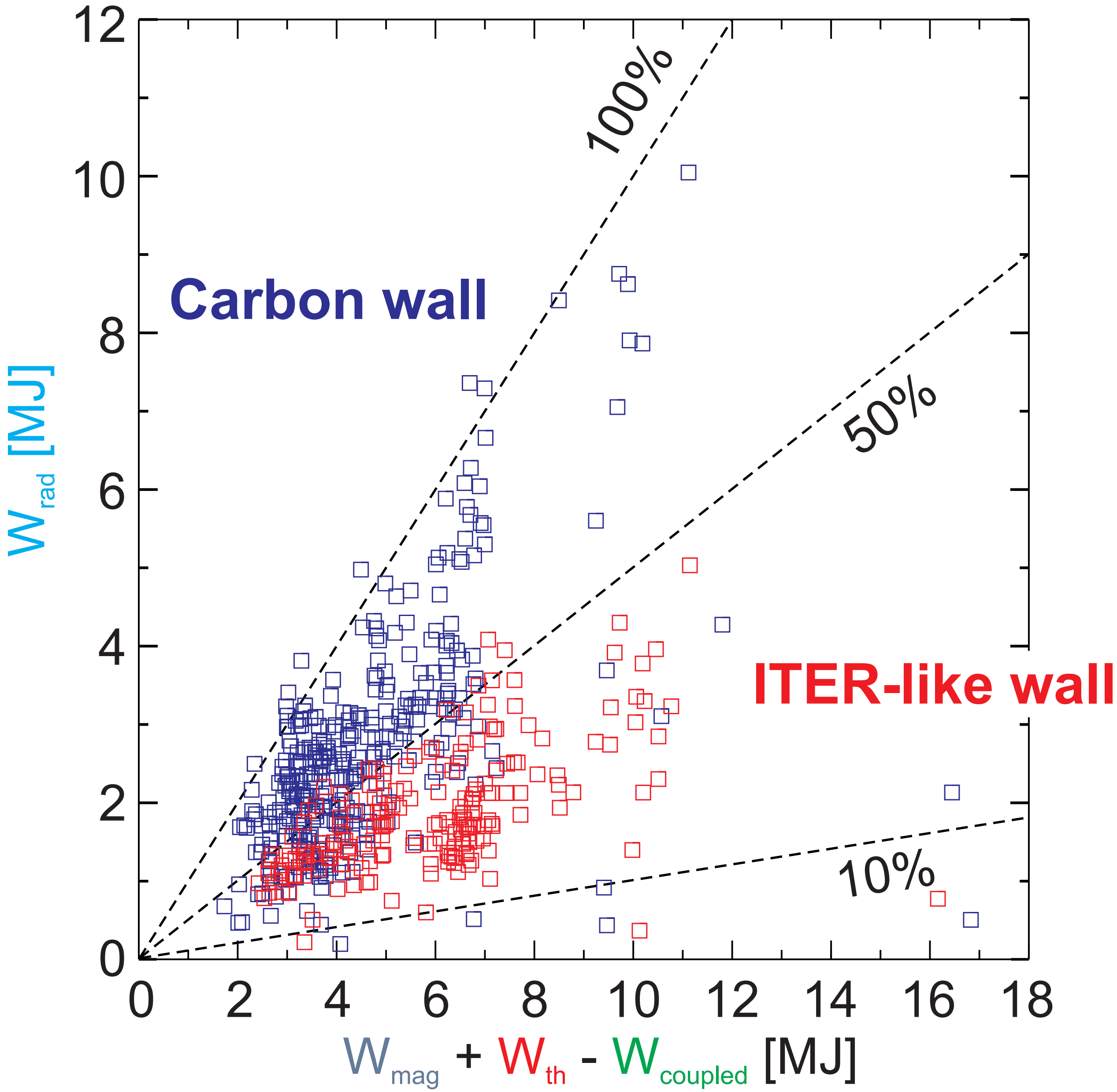

ITER-like wall

Radiation

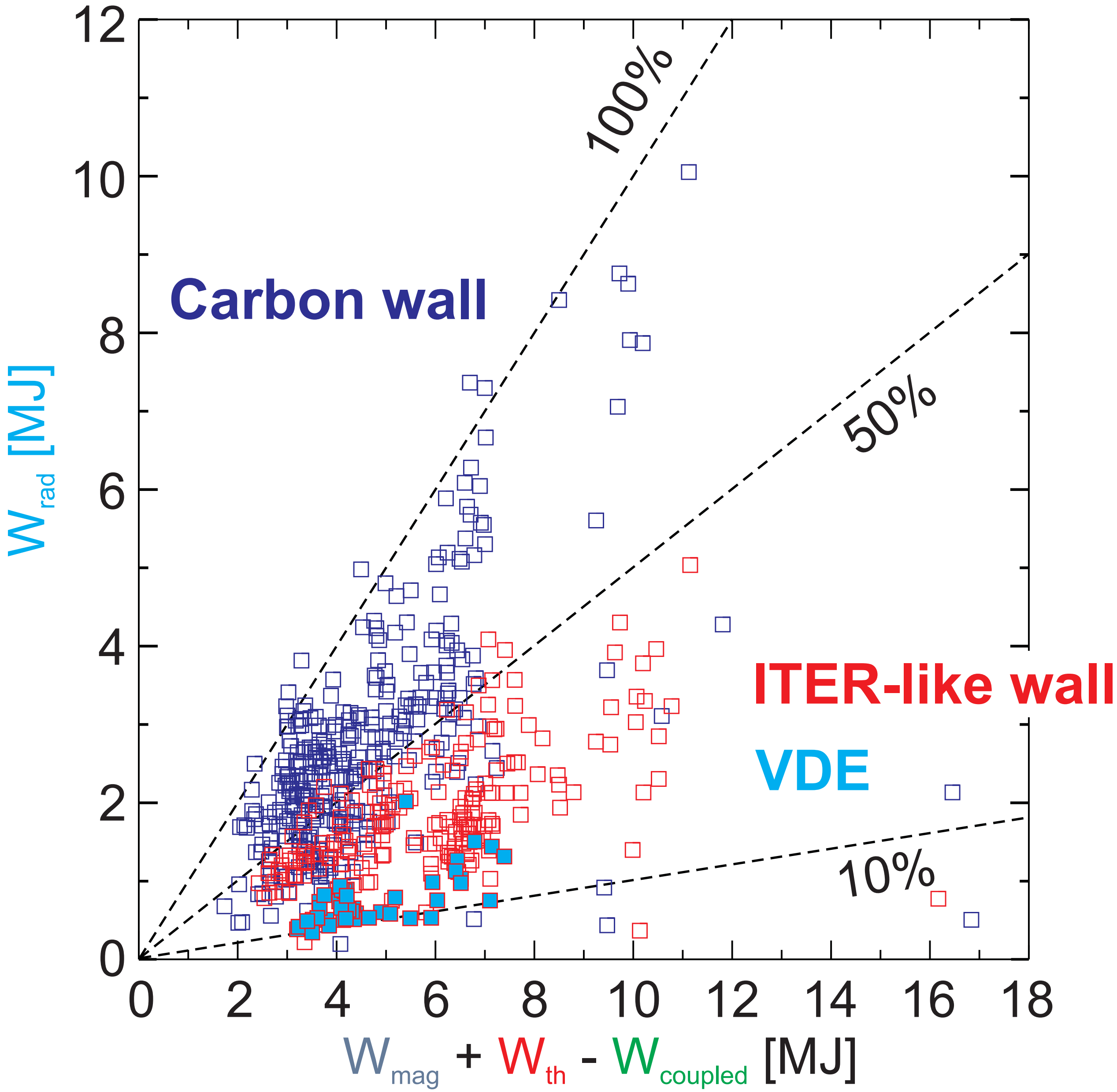

12
10
8
6
4
2
0
0
2
4
6
8
10
12
14
16
18
100%
50%
10%
Carbon wall
ITER-like wall
VDE
W rad [MJ]
W mag + W th - W coupled [MJ]

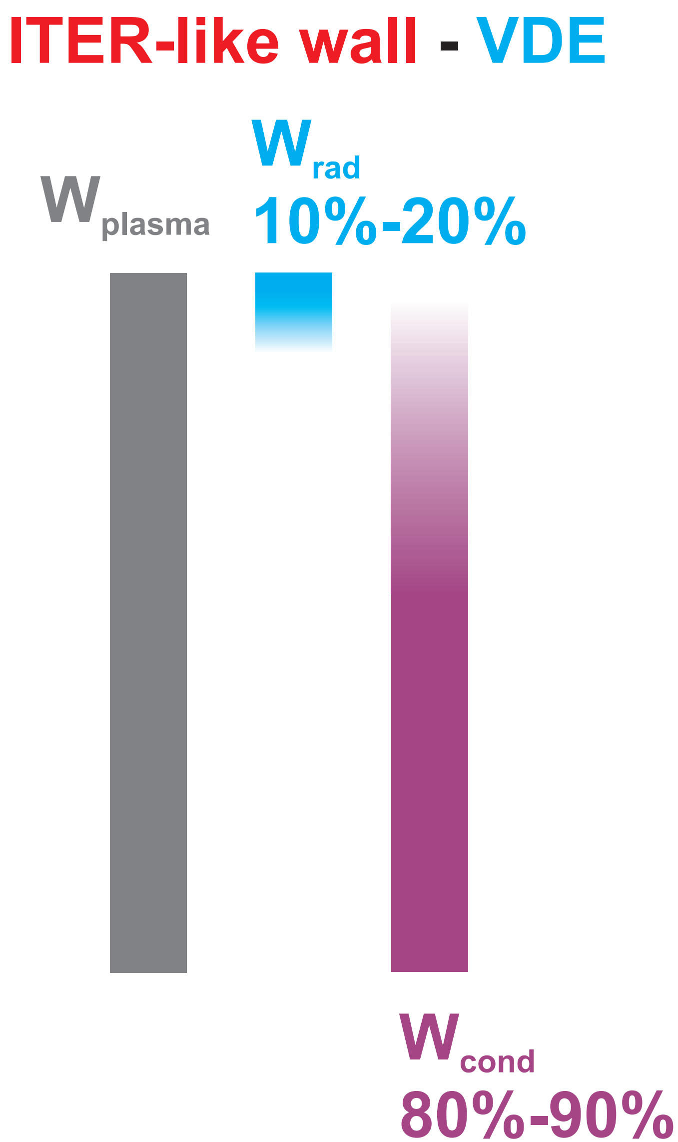

ITER-like wall - VDE
W plasma
W rad
10%-20%
W cond
80%-90%

Timescales

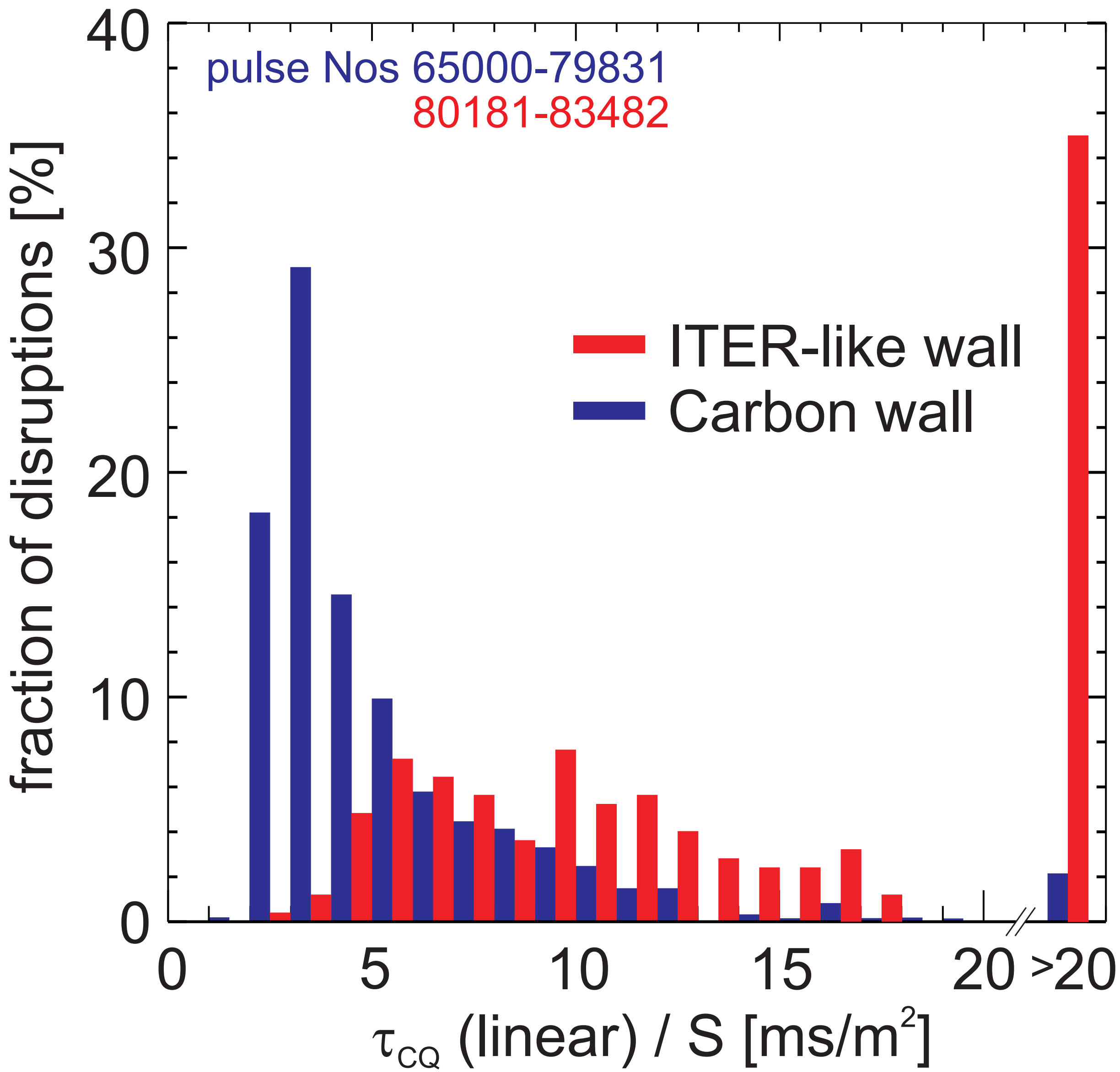

Carbon wall

current quench time determined by the radiation loss time

ITER-like wall

current quench time determined by the transport / vertical growth time

no runaway electrons formation

⇨ V.V. Plyusnin, V.G. Kiptily et al. EX/P8-05

Electro-magnetic loads

Electro-magnetic loads arise from

eddy currents

vertical force

halo currents

vertical force

rolling motion

toroidal current asymmetries

sideways force

radial displacement

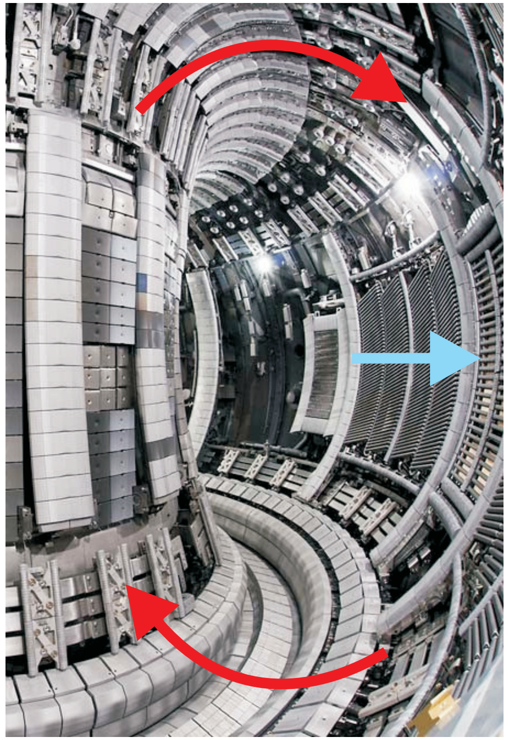

Electro-magnetic loads

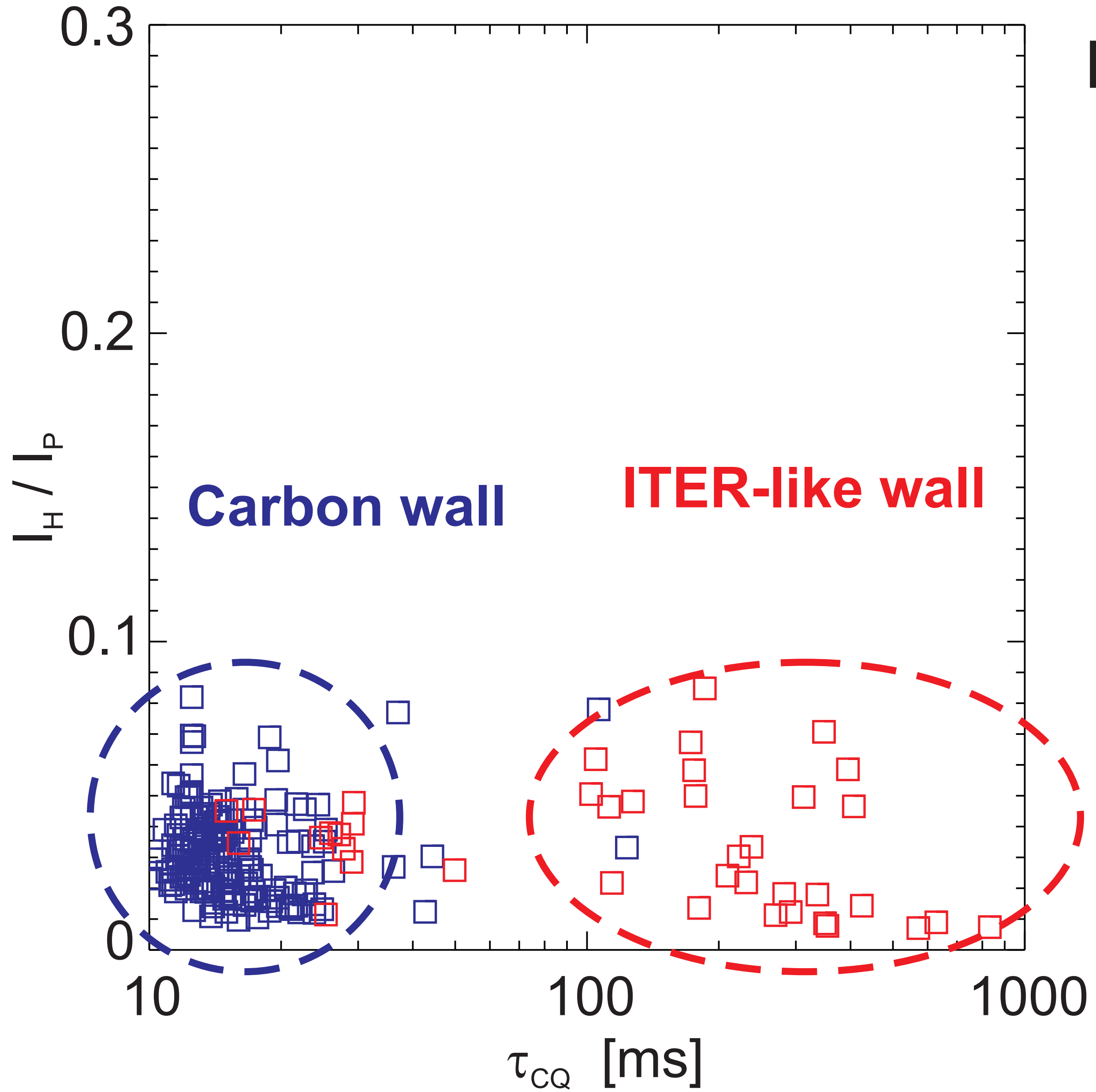

Halo currents

small vertical displacement

open symbols: $\Delta z < 0.4$m at 70%I_P

Electro-magnetic loads

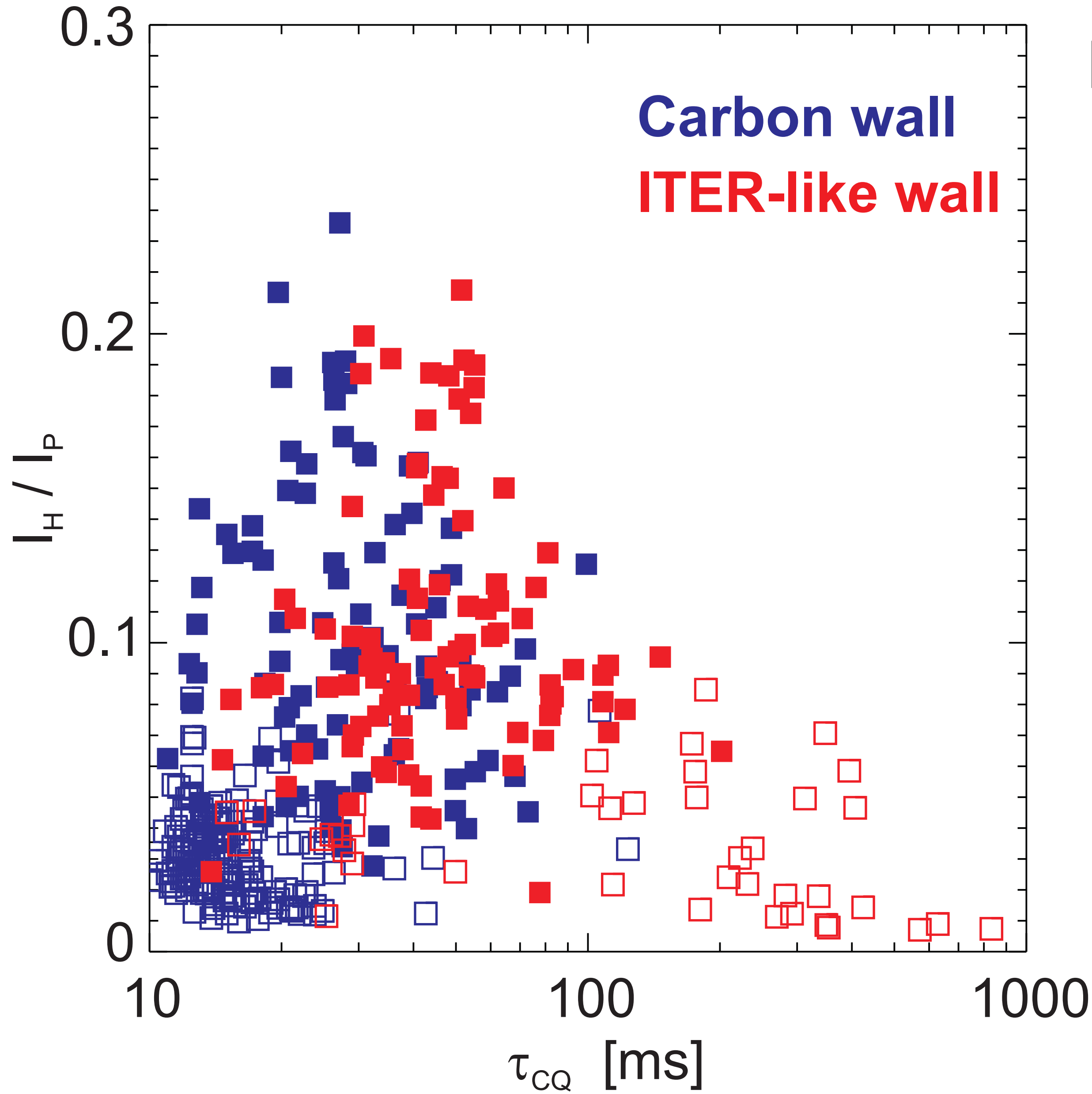

Halo currents

large vertical displacement

closed symbols: $\Delta z > 0.4$m at 70%I_P

Electro-magnetic loads

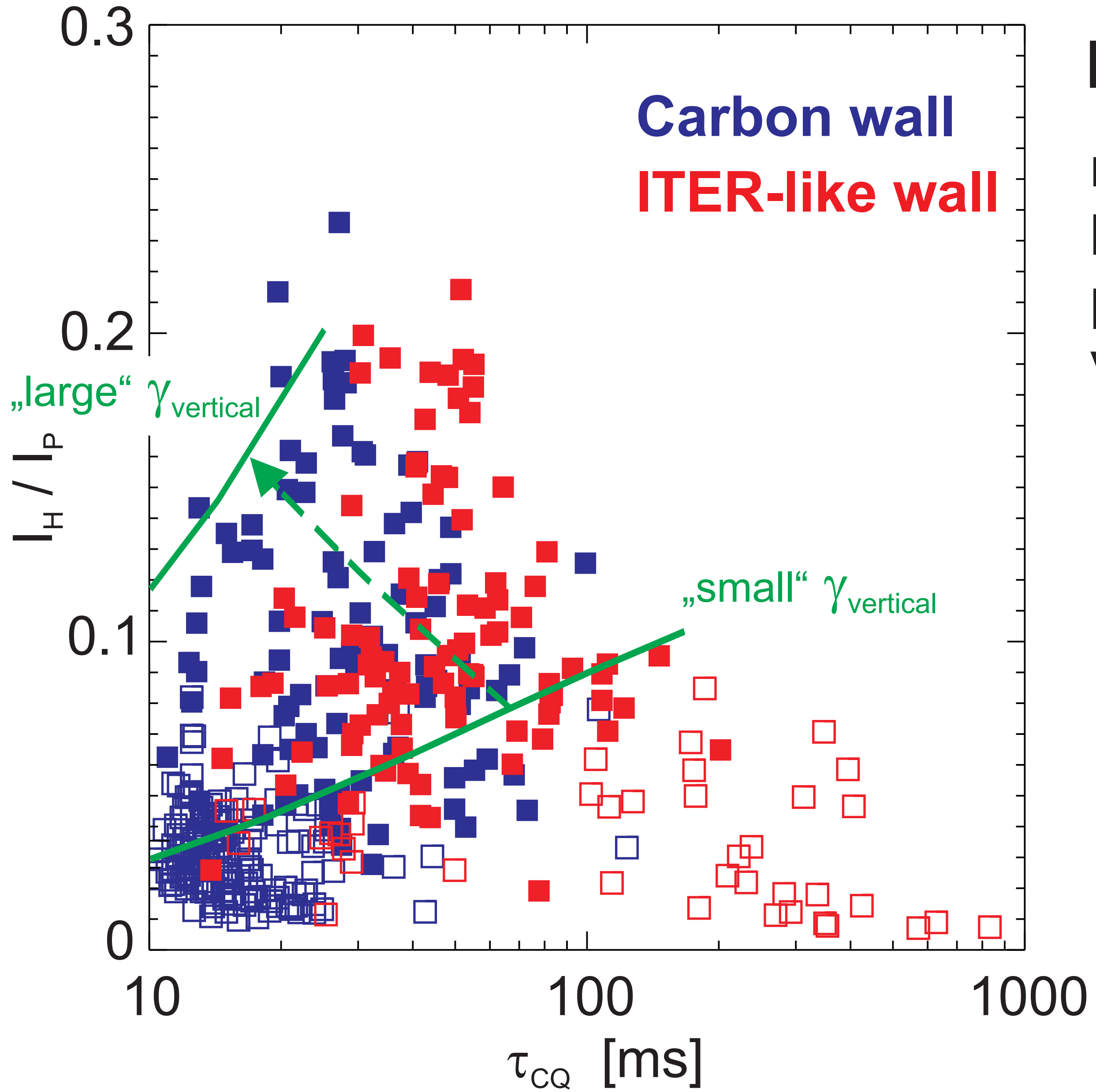

Halo currents

maximum I_{halo} determined by competition between plasma resistive timescale and vertical growth rate

large vertical displacement

closed symbols: $\Delta z > 0.4$m at 70%I_P

Electro-magnetic loads

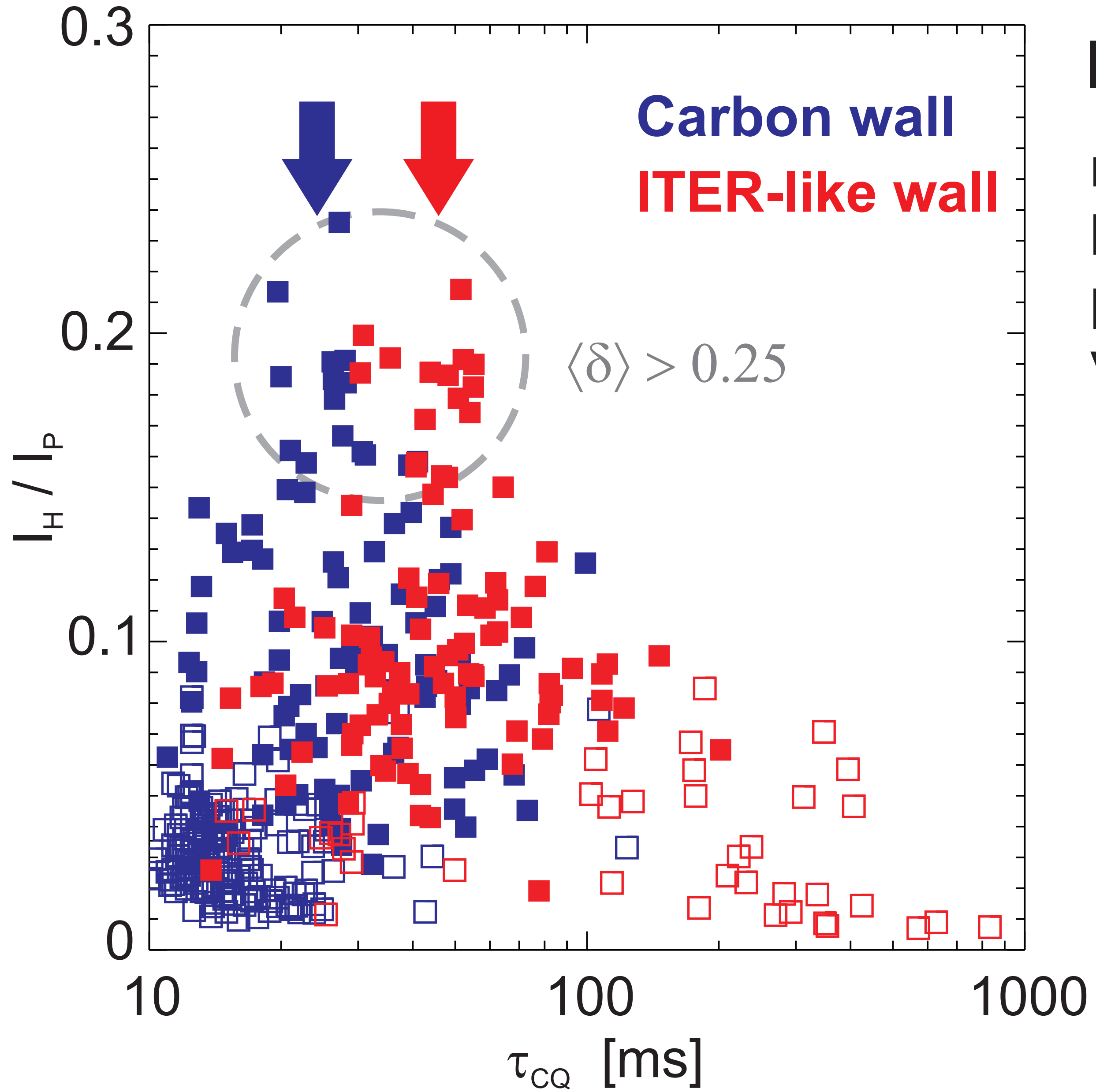

Halo currents

maximum I_{halo} determined by competition between plasma resistive timescale and vertical growth rate

large vertical displacement

closed symbols: Δz > 0.4m at 70%I_P

ITER-like wall:

peak I_H/I_P at longer τ_{CQ}

Electro-magnetic loads

vessel displacement increases with impulse

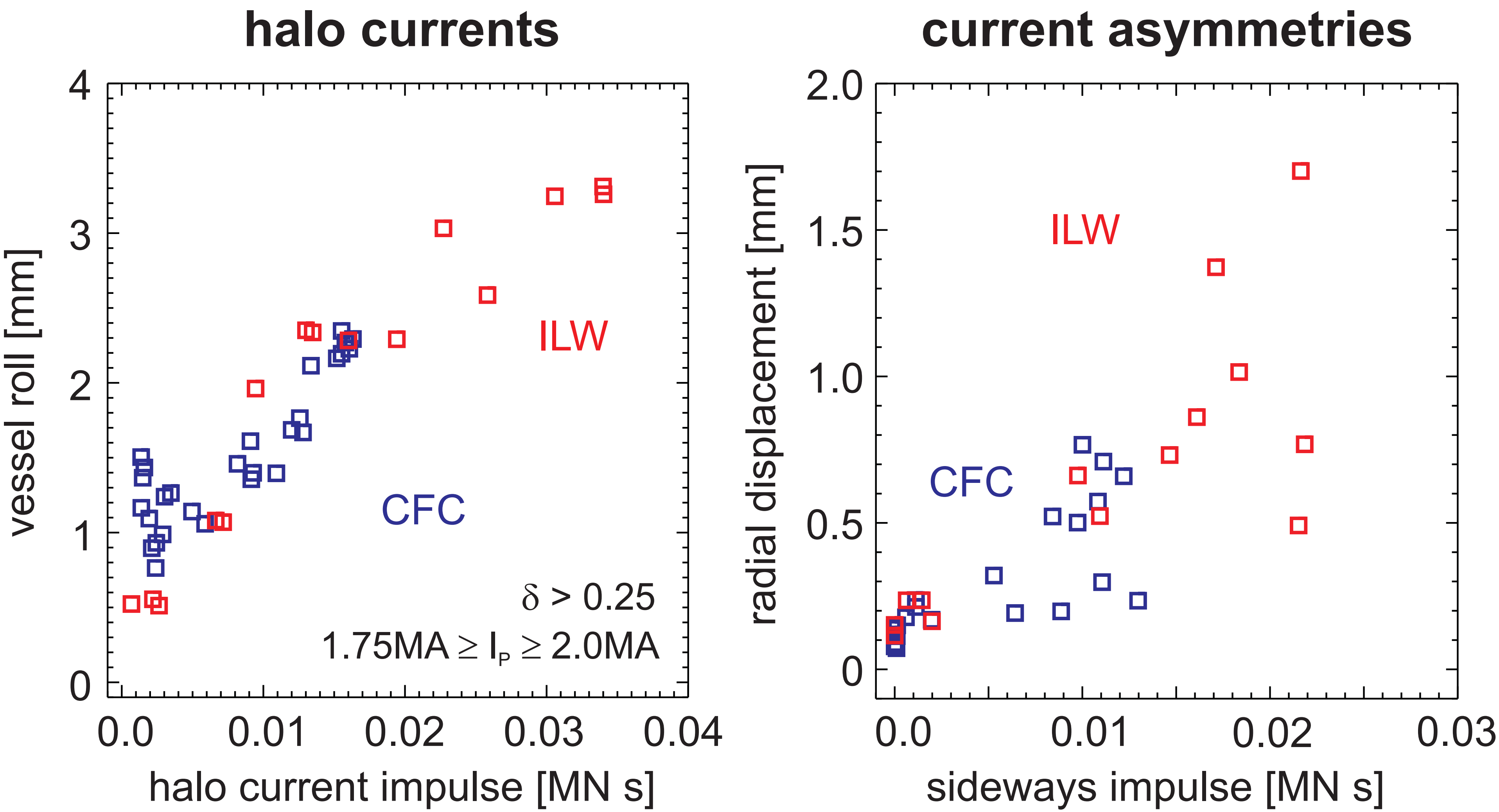

Electro-magnetic loads

vessel displacement increases with impulse

halo currents

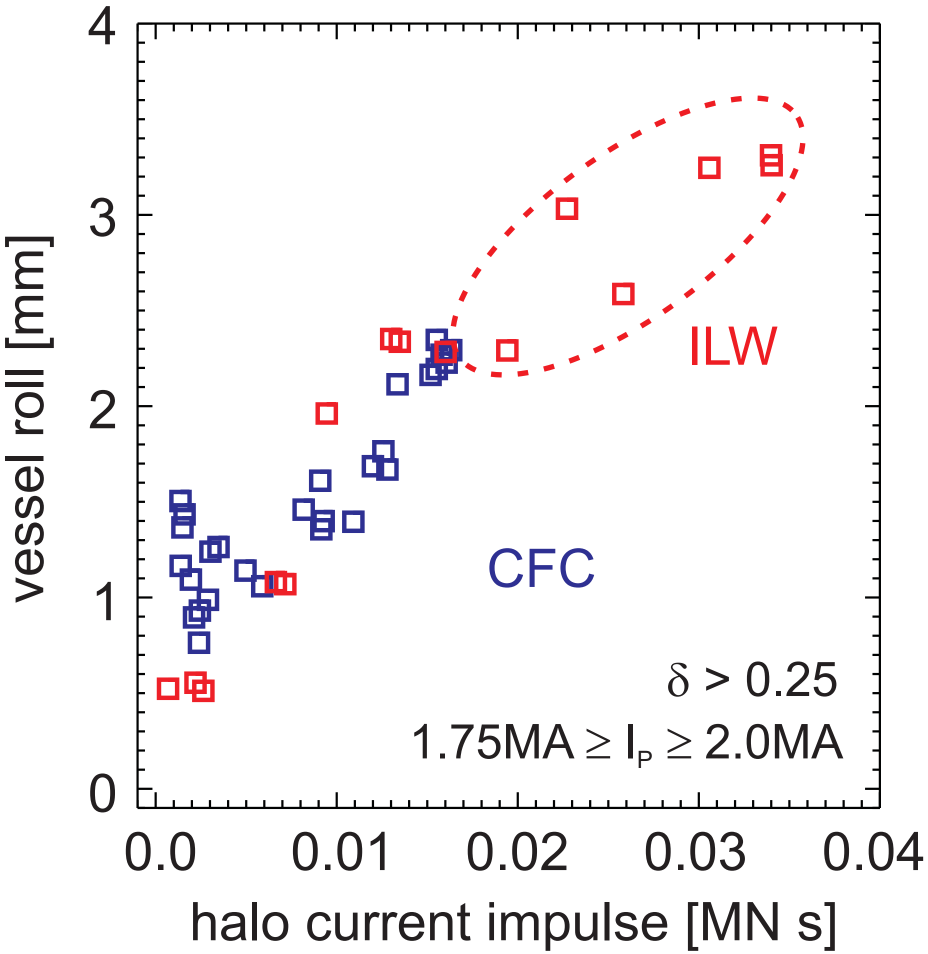

current asymmetries

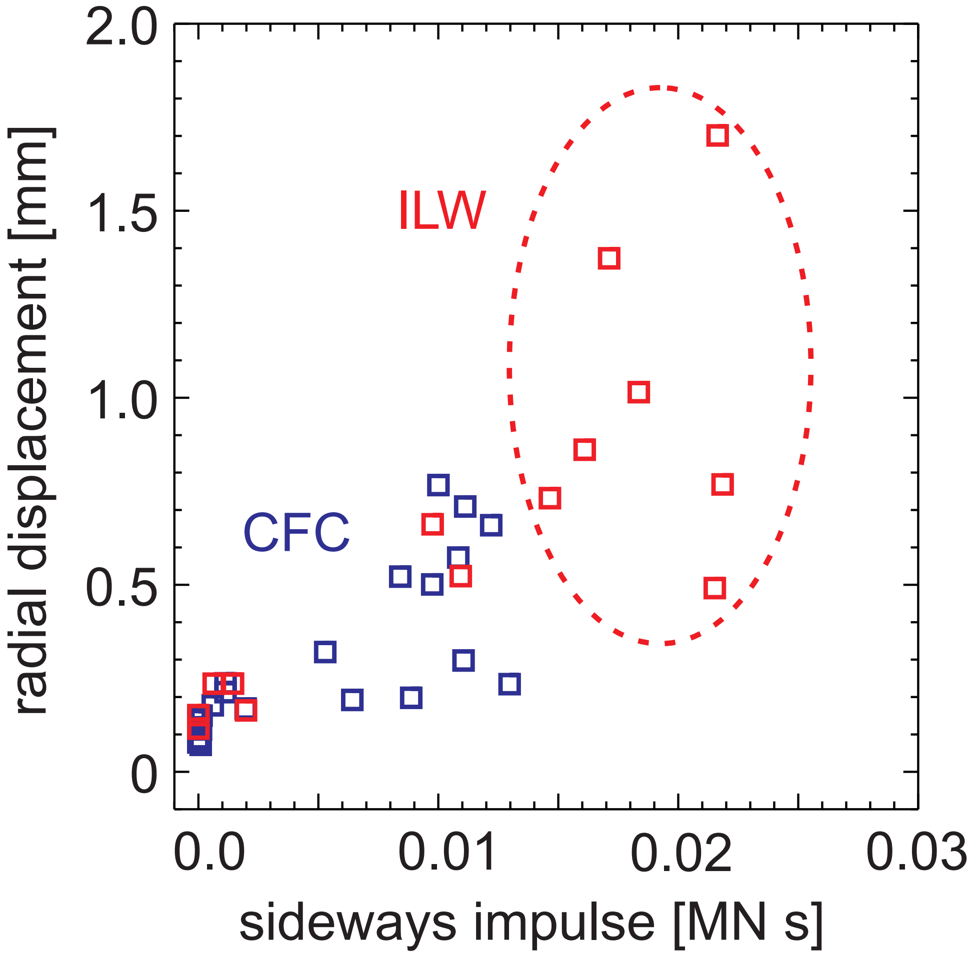

Heat Loads

CQ-VDE deposits high fraction of W_{mag} on upper PFCs

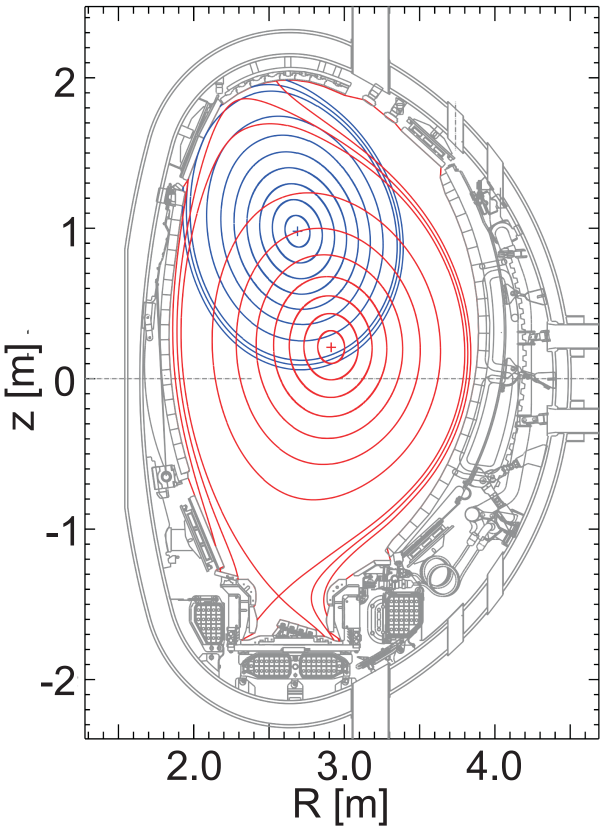

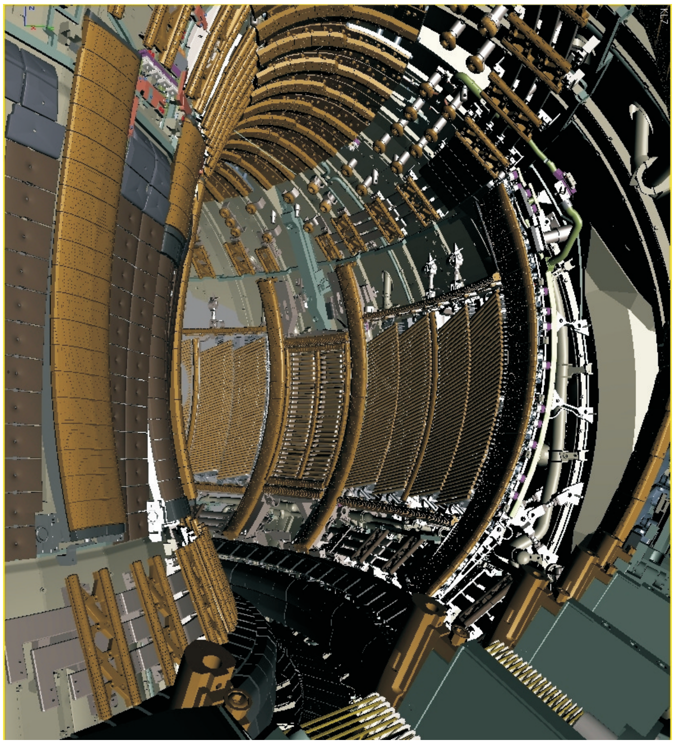

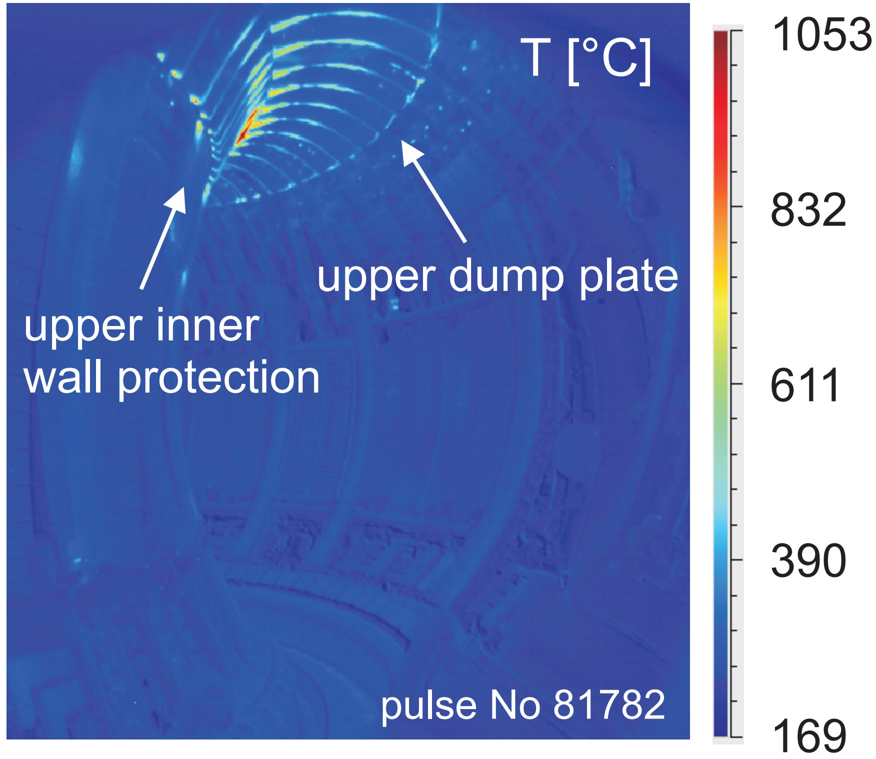

maximum temperature ~**1050°C**

(slow time resolution of 20ms)

modest magnetic energy: W_{mag} = 14.3MJ (2.2MA)

low thermal energy: W_{th} = 1.5MJ

Heat Loads

CQ-VDE deposits high fraction of W_{mag} on upper PFCs

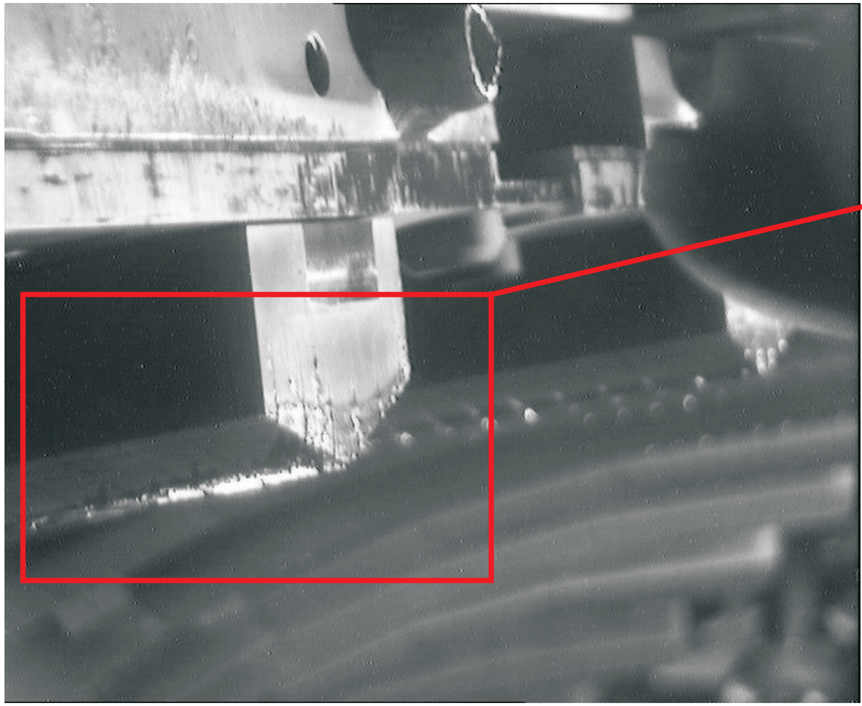

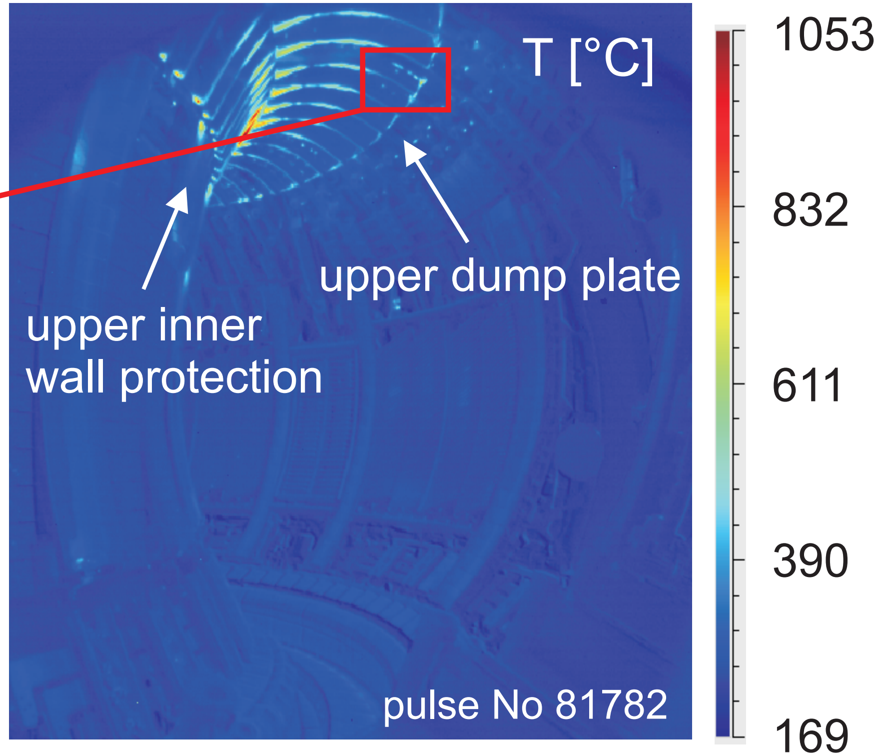

maximum temperature ~**1050°C**
(slow time resolution of 20ms)

modest magnetic energy: W_{mag} = 14.3MJ (2.2MA)
low thermal energy: W_{th} = 1.5MJ

Heat Loads

Heat load impact during current quench

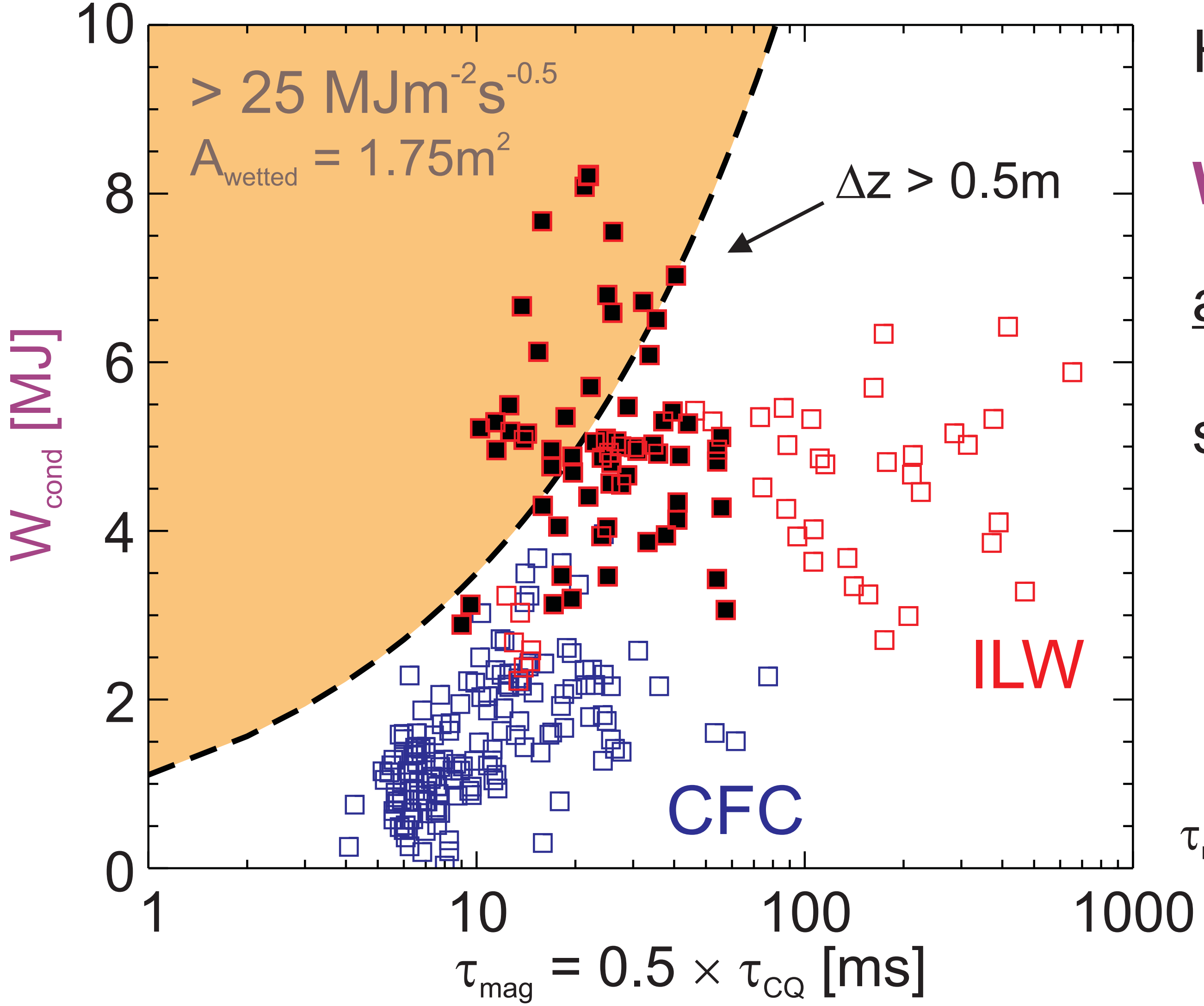

Heat loads increase with

$W_{cond} = W_{mag} + W_{th} - W_{coupled} - W_{rad}$

and

shorter deposition time

$$\Delta T \sim W \times A^{-1} \times \tau^{-0.5}$$

τ_{mag}: upper limit of deposition time

Heat Loads

Heat load impact during current quench

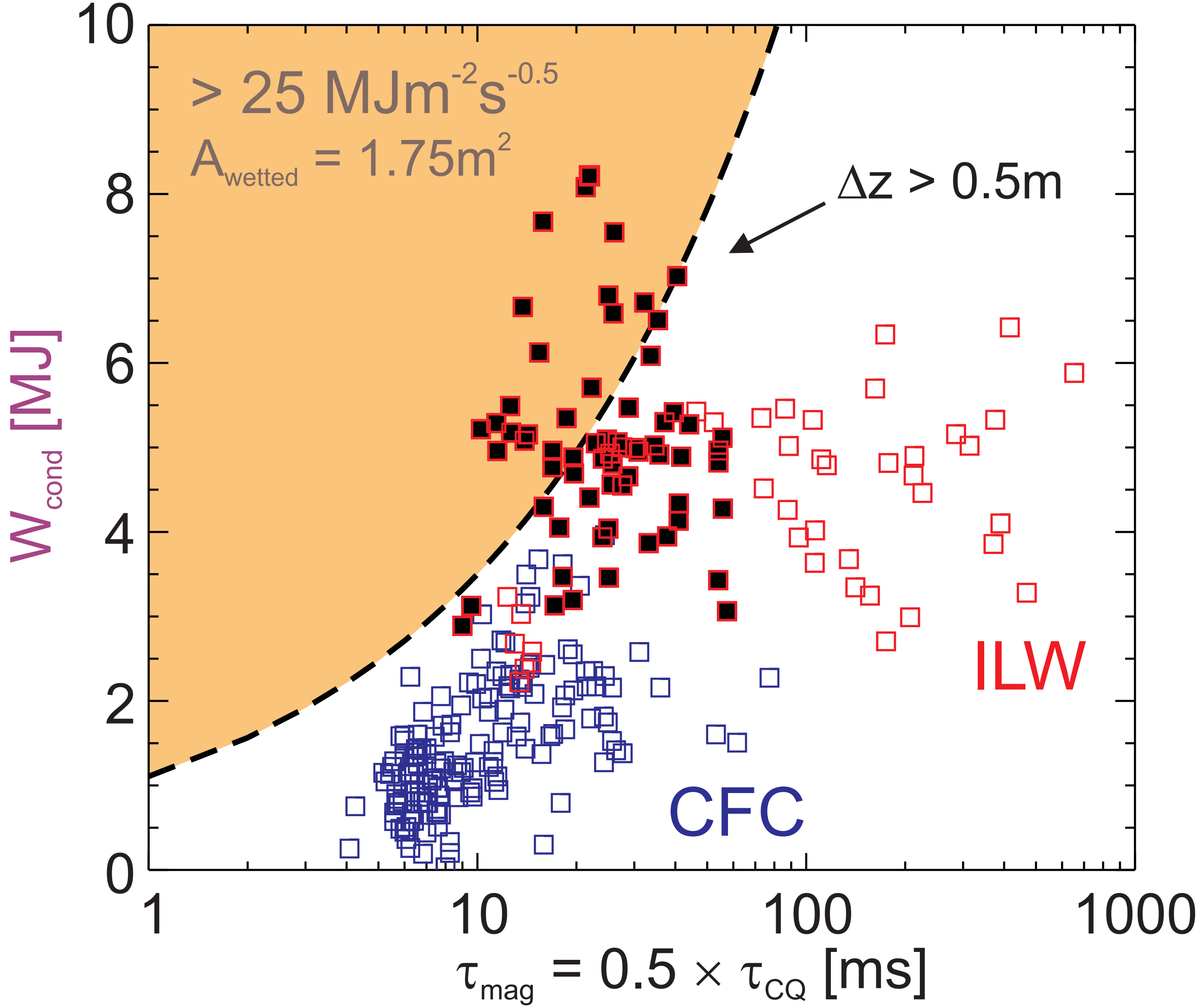

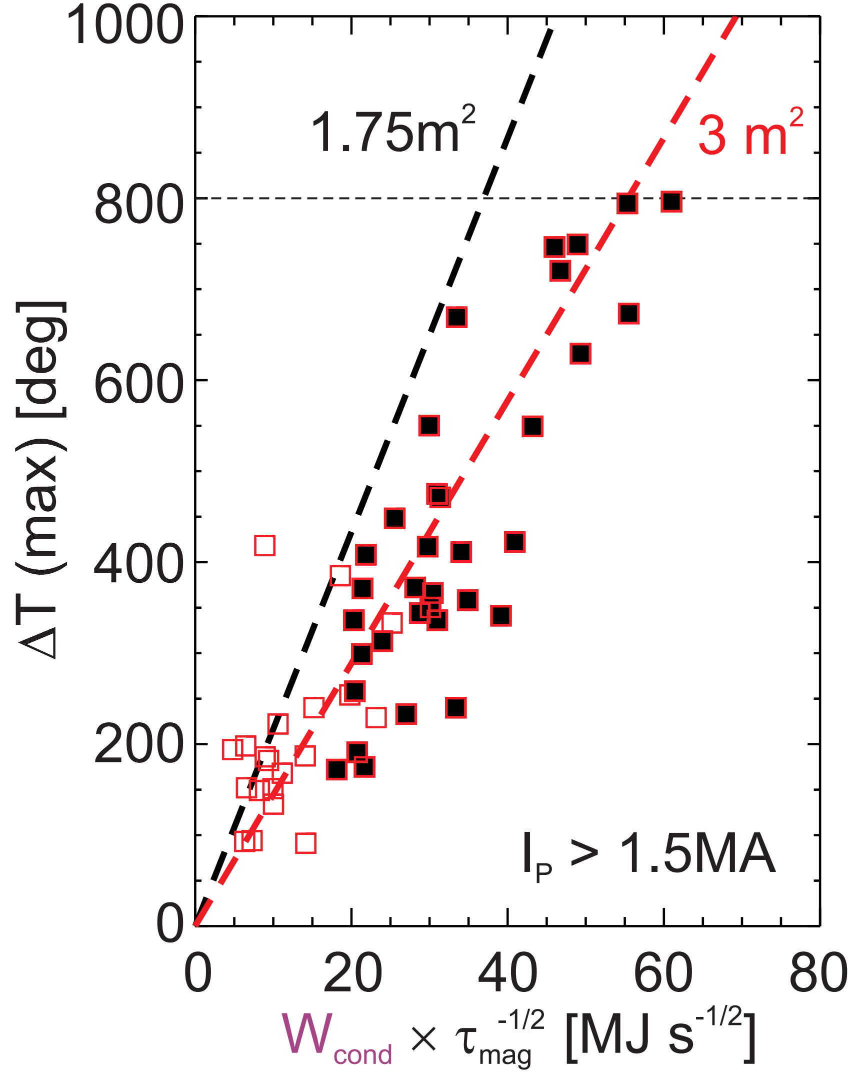

Massive Gas Injection (MGI)

injected species

He, D_2, Ne, Ar, 10%Ar or 10%Ne in D_2

number of particles injected before TQ

$0.1 - 20 \times 10^{22} \approx 0.2 - 40 \times N_e$

MGI is applied now with the ILW in closed loop for $I_P \geq 2.5$MA

⇨ E. Joffrin et al. EX/1-1

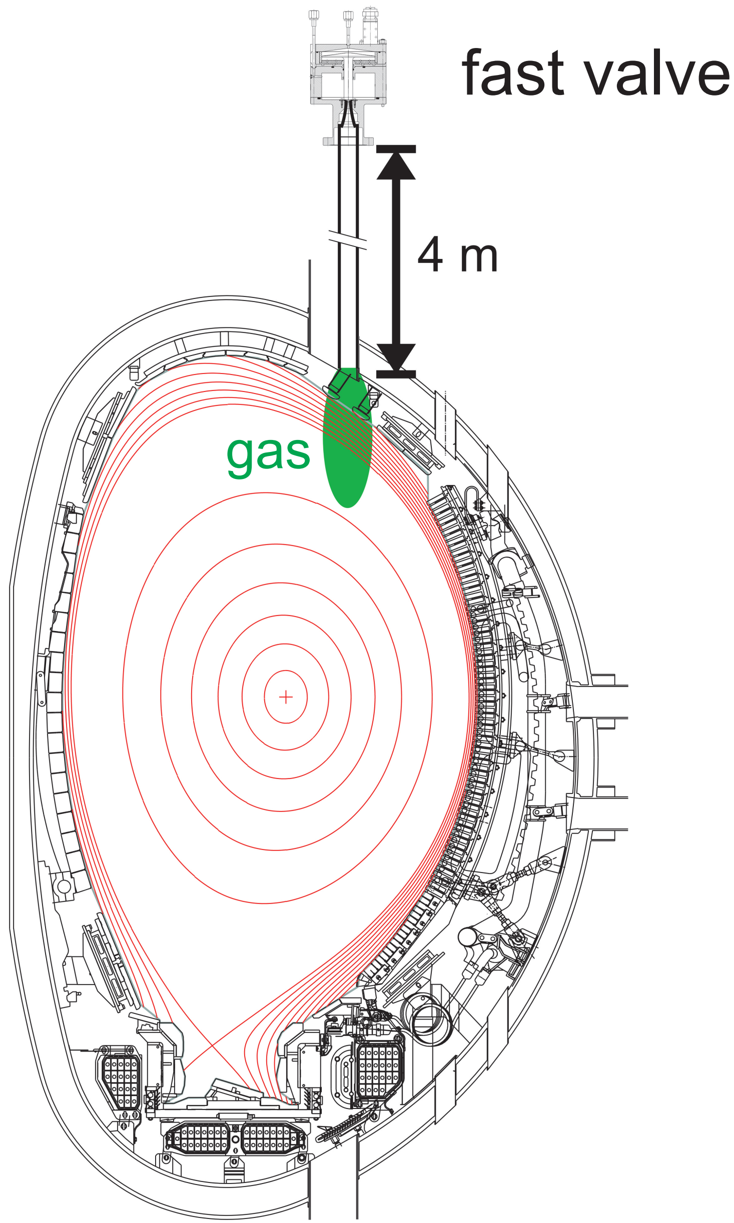

MGI - Radiation

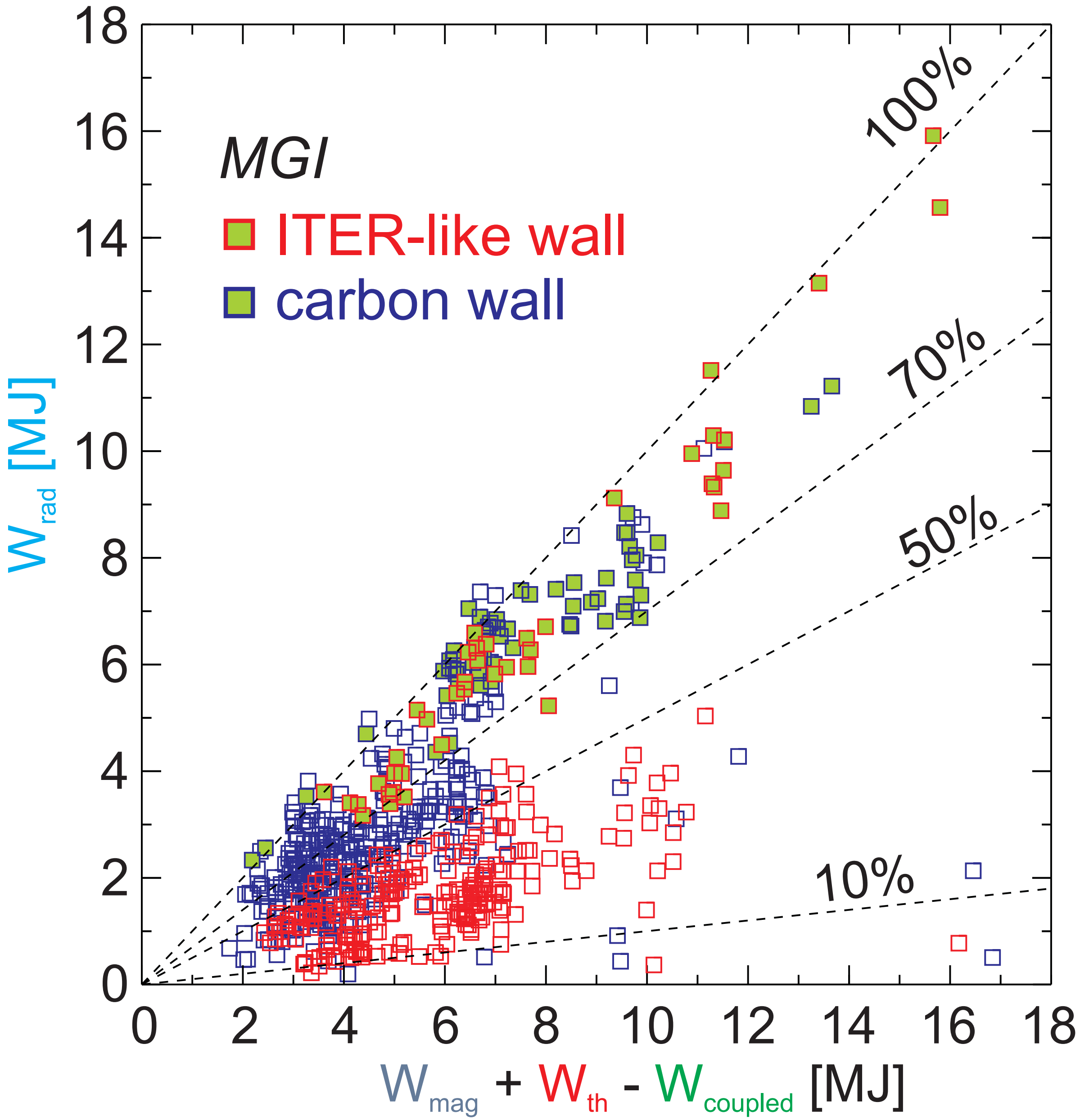

high level of radiation

W_{rad} / W_{plasma} ~ 70% and 100%

Scatter

species, injection rate, timing

MGI - Timescales

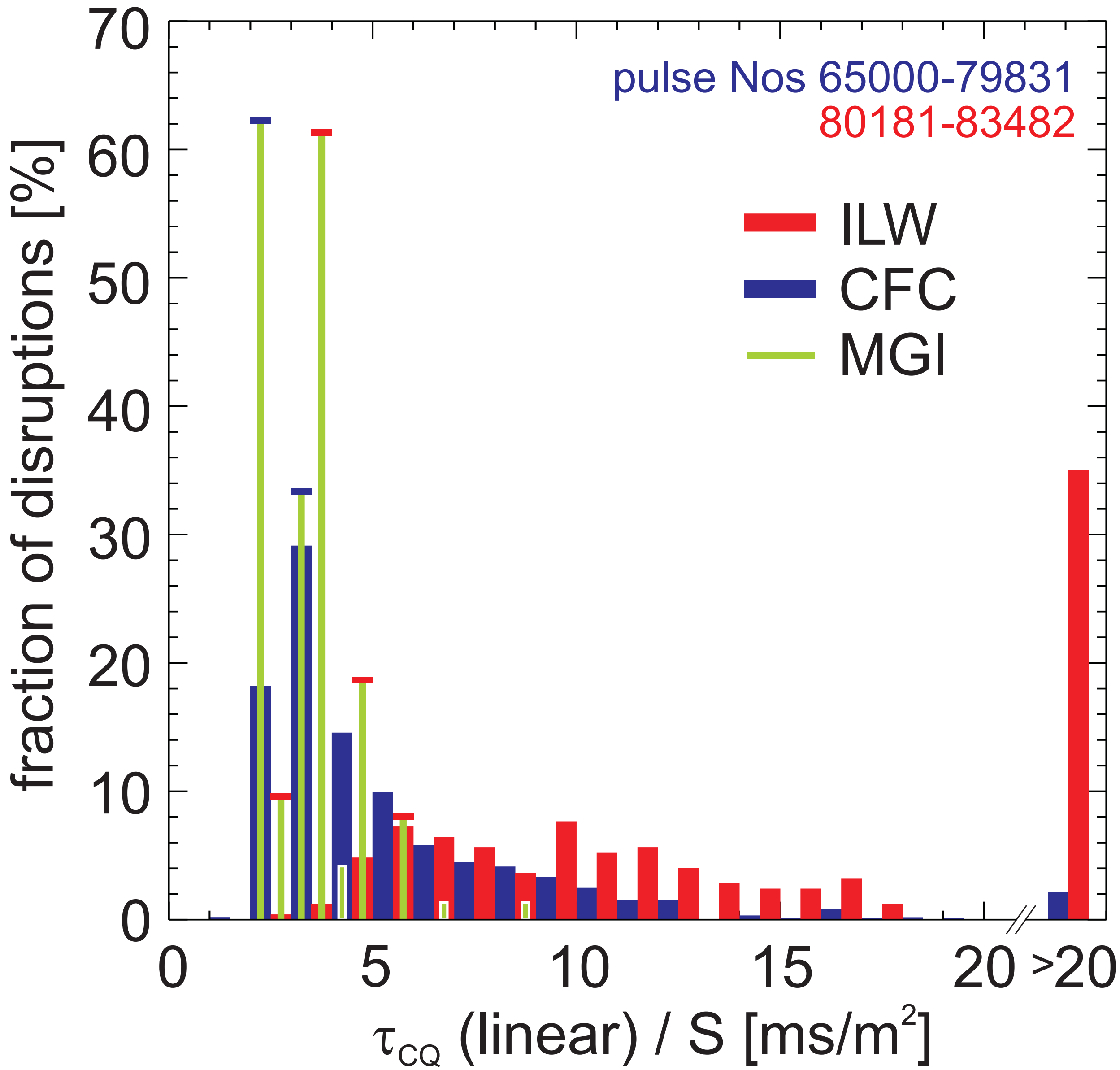

short current quench times

ILW

tendency towards longer τ_{CQ}

MGI - Electro-magnetic loads

halo and sideways impulse negligible / force from eddy currents remains

halo currents

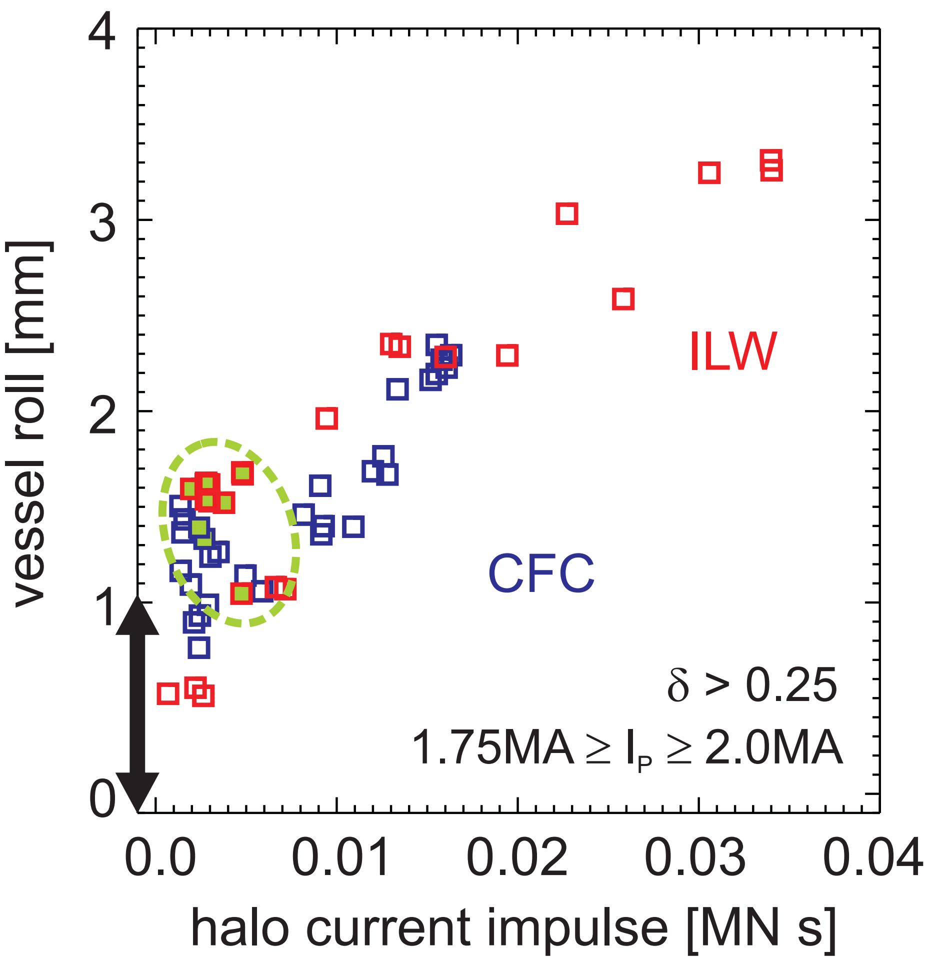

current asymmetries

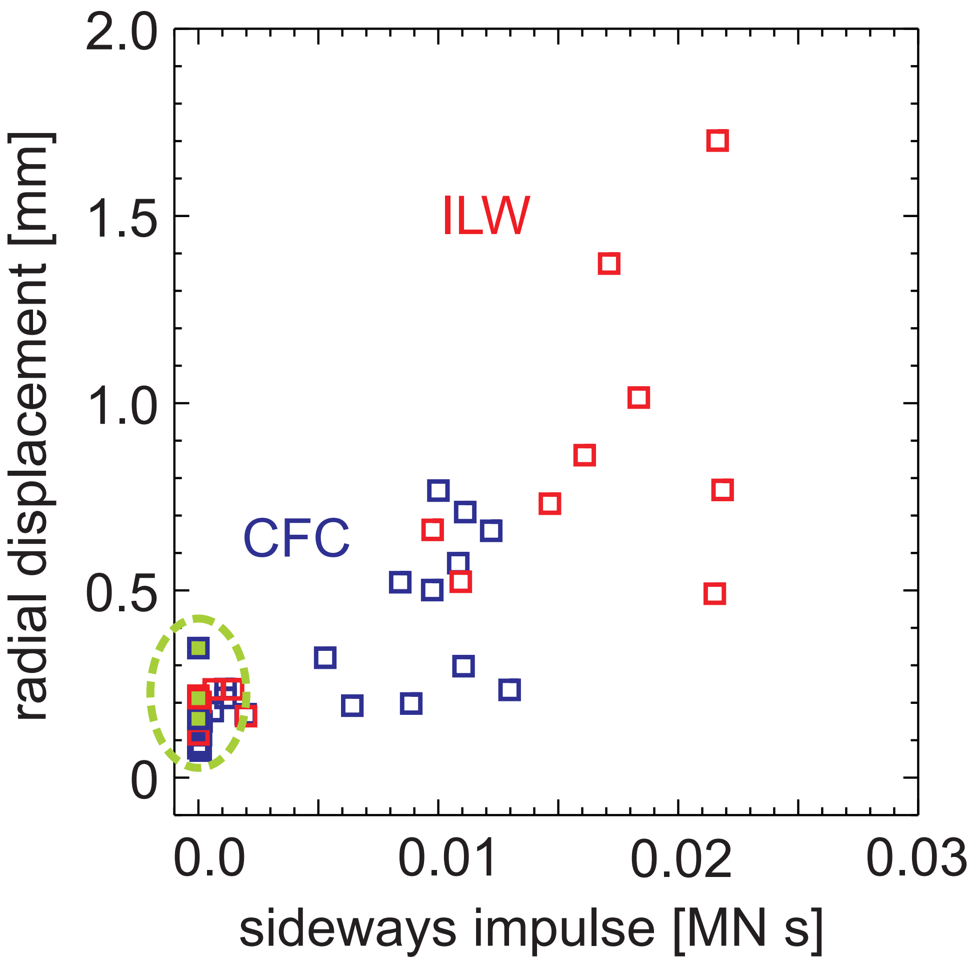

MGI - Heat loads

heat loads reduced due to high W_{rad}

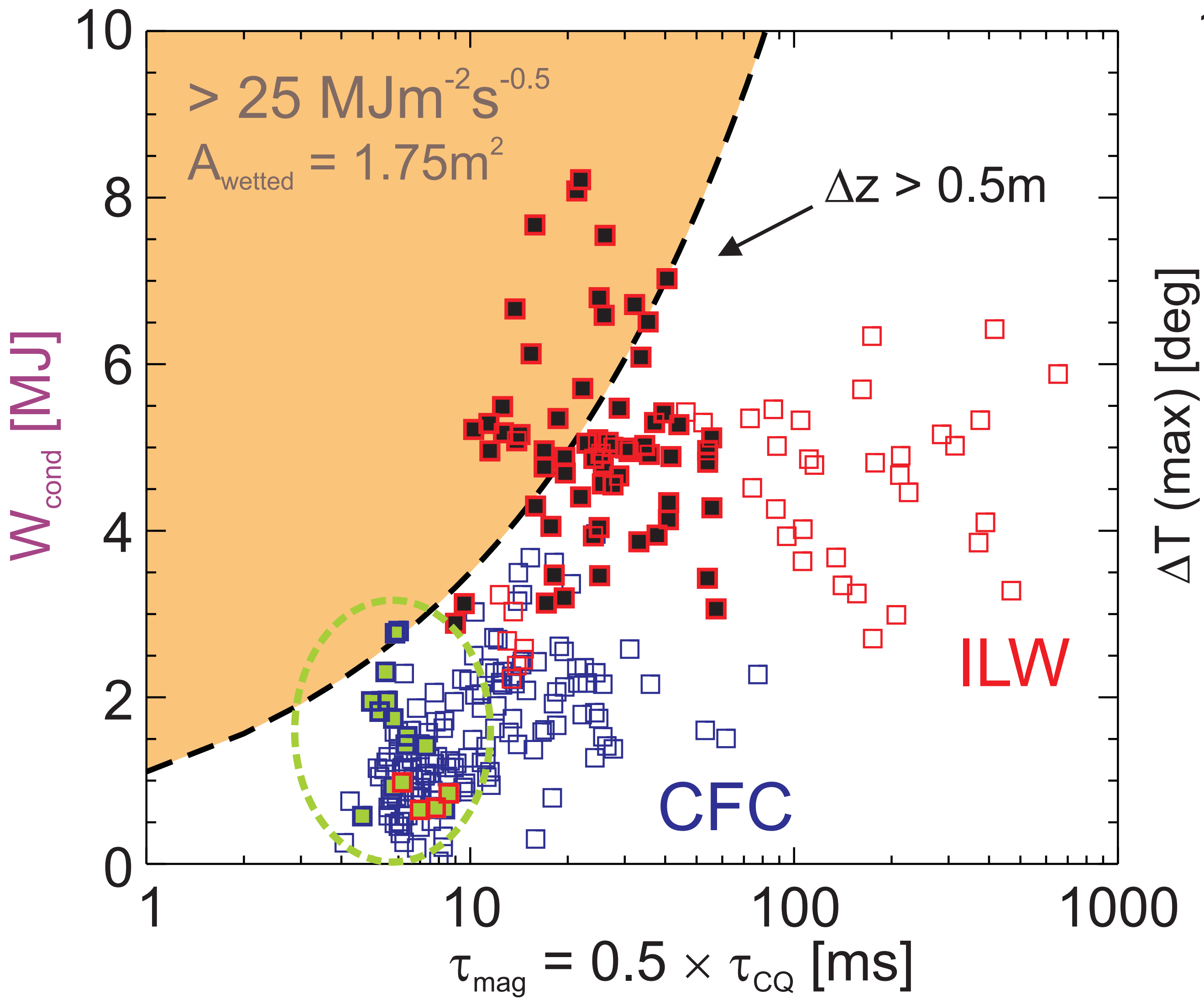

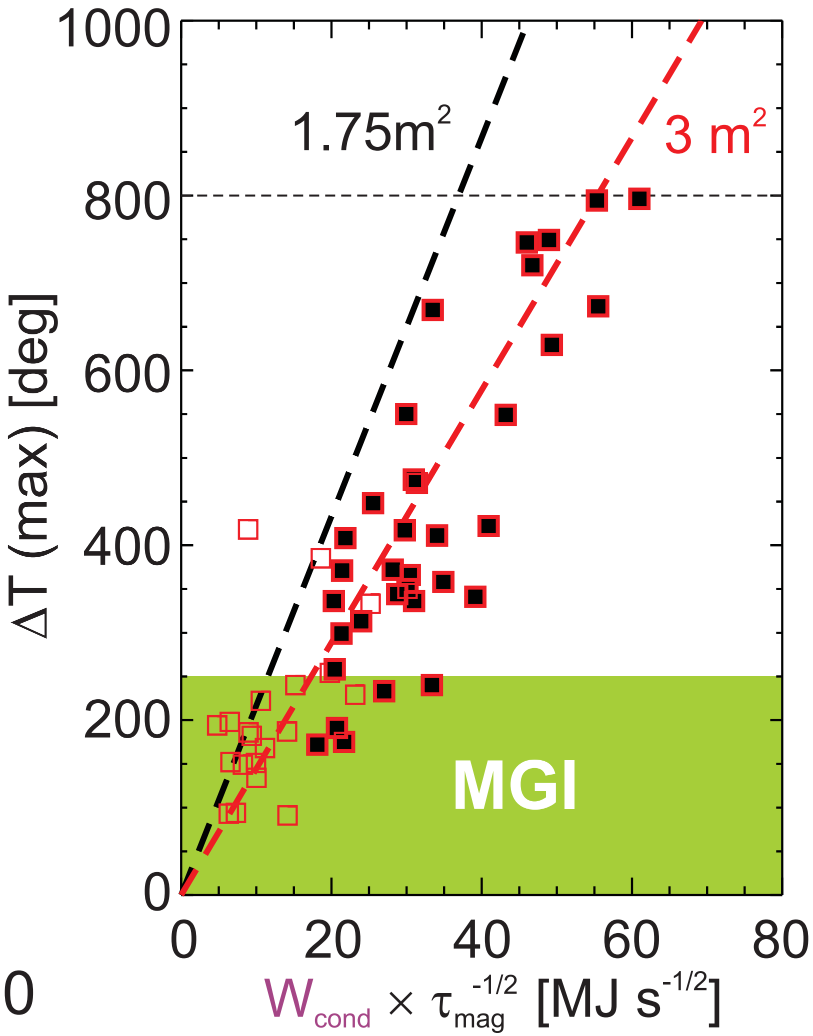

MGI - Radiation efficiency

Radiation efficiency with increasing thermal energy

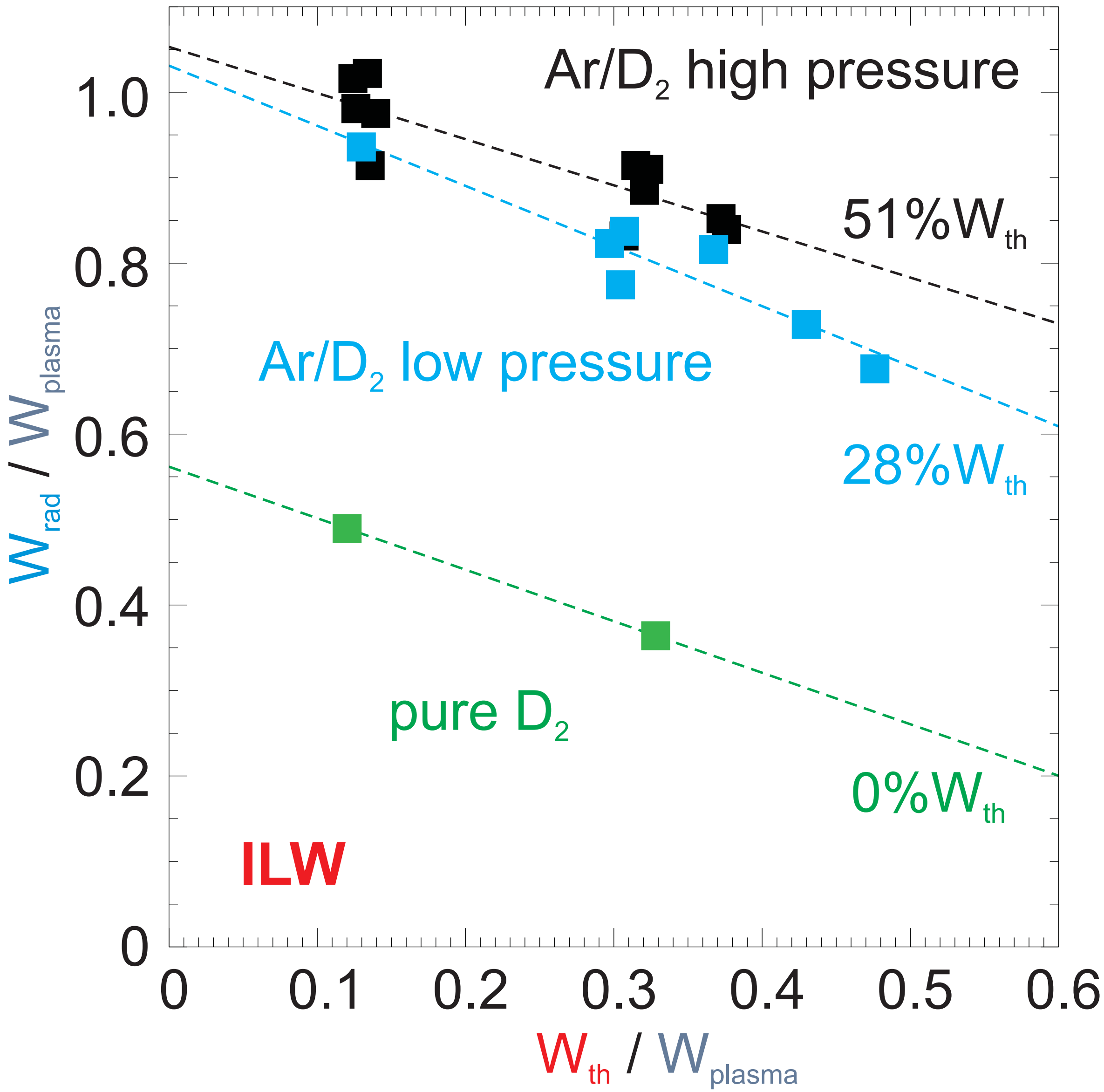

High radiation fraction up to 100% with $Ar+D_2$ for ohmic pulses

Low radiation for D_2

Thermal quench:

low radiation efficiency

high pressure: $N^{Ar}_{inj,CQ} \approx 4\times10^{21}$

Disruptions with the ITER-like wall - What have we learned for ITER so far?

Radiation

- without carbon PFCs ⟹ low radiation
- energy dissipation through conduction/convection dominates

Loads

- magnetic energy contributes significantly to heat loads (in addition to TQ)
  $W_{mag} \leq 500$ MJ (ITER, 15MA, inside VV)
- stresses on vessel are increased due to longer impact of forces

Mitigation

- Massive gas injection controls radiation level
- 10%Ar in D_2 efficiently mitigates heat loads and electro-magnetic loads

  MGI is now mandatory in JET for $I_P \geq 2.5$MA

- low mitigation efficiency during thermal quench (ITER requires > 90%)

  location of injection, scaling with injected amount?

  ➡ 2^{nd} valve at outer midplane in 2013

Impact and mitigation of disruptions with the ITER-like wall in JET

M. Lehnen[1], G. Arnoux[2], S. Brezinsek[1], J. Flanagan[2], S.N. Gerasimov[2], N. Hartmann[1], T.C. Hender[2], A. Huber[1], S. Jachmich[3], U. Kruezi[2], G.F. Matthews[2], J. Morris[2], V.V. Plyusnin[4], C. Reux[5], V. Riccardo[2], B. Sieglin[6], P. de Vries[7] and JET EFDA contributors*

JET-EFDA, Culham Science Centre, Abingdon, OX14 3DB, UK

[1]Institute of Energy and Climate Research - Plasma Physics, Forschungszentrum Jülich, Association EURATOM-FZJ, Trilateral Euregio Cluster, 52425 Jülich, Germany

[2]Euratom/CCFE Association, Culham Science Centre, Abingdon, Oxon, OX14 3DB, UK

[3]Laboratoire de Physique des Plasmas-Laboratorium voor Plasmafysica, Association EURATOM-Belgian State, ERM/KMS, B-1000 Brussels, Belgium

[4]Instituto de Plasmas e Fusão Nuclear/IST, Associacao EURATOM-IST, Av. Rovisco Pais, 1049-001 Lisbon, Portugal

[5]École Polytechnique, LPP, CNRS UMR 7648, 91128 Palaiseau, France

[6]Max-Planck-Institut für Plasmaphysik, EURATOM-Assoziation, 85748 Garching, Germany

[7]FOM institute DIFFER, Association EURATOM-FOM, P.O.Box, 1207, 3430BE, Netherlands

*see the Appendix of F. Romanelli et al., Proceedings of the 24th IAEA Fusion Energy Conference 2012, San Diego, US